International Journal of Climatology

International Journal of Climatology | RMetS

RESEARCH ARTICLE OPEN ACCESS

Characteristics of Intense Multi-Day Wet Spells Over West Africa

Oluwaseun. W. Ilori[1,2,3,4] | Marlon Maranan[2] | Andreas H. Fink[2] | Zachariah D. Adeyewa[1,3]

[1]Department of Meteorology and Climate Science, Federal University of Technology, Akure, Nigeria | [2]Karlsruhe Institute of Technology, Karlsruhe, Germany | [3]WASCAL Graduate Research Programme in West African Climate System, Federal University of Technology, Akure, Nigeria | [4]Department of Meteorology and Climate Change, Nigeria Maritime University, Okerenkoko, Nigeria

Correspondence: Oluwaseun. W. Ilori (hilorywilson@gmail.com)

Received: 20 December 2024 | **Revised:** 11 November 2025 | **Accepted:** 10 December 2025

Keywords: characteristics of wet spells: frequency, intensity and size | extreme and intense wet spells | West Africa rainfall

ABSTRACT

This study examines the characteristics of intense multi-day wet spells in West Africa, which have significant socioeconomic impacts but remain understudied, using rain gauge and satellite-based rainfall data from 1982 to 2020. A gridded dataset, developed from the Karlsruhe African Surface Station-Database (KASS-D) using the SPHEREMAP interpolation method with data from 239 rain-gauging stations was compared with GPCC, CHIRPS and IMERG datasets. Wet days (rainfall > 1.0 mm) were aggregated into 3-day and 5-day events, with the 90th percentile threshold identifying intense wet spells. The quantile distribution of wet-day rainfall amounts in KASS-D aligns closely with GPCC, CHIRPS and IMERG datasets, although discrepancies occur at the tails of the distribution. KASS-D and the arithmetic mean of station data show similar quantile distributions when grid pixels contain 1–4 stations, but KASS-D values increase with more than four stations per pixel. The analysis reveals a latitudinal variation in wet spell frequency, with 5-day events often extending from 3-day events, peaking in June and September along the Guinea Coast and in August in other climatic zones. Over the course of the study period, the frequency of intense wet spells increased significantly, particularly in KASS-D, highlighting the added value of dense rain gauge networks in creating reanalysis and improving satellite rainfall products. Spatially large-sized intense events, along with average and maximum sizes, have increased, while small and medium-sized events have declined significantly (both in GPCC and CHIRPS), leading to a greater contribution of 3-day and 5-day wet spells to annual rainfall. The Guinea Coast experienced the highest increase in percentage contribution, while the Sahel saw the lowest. This study underscores the rising intensity, size and contribution of multi-day wet spells to annual rainfall in West Africa, emphasising the need for high-quality rain gauge networks and a deeper understanding of the dynamics driving these events.

1 | Introduction

Rainfall is a critical climatic parameter for assessing climate change and variability, especially in West Africa, where it exhibits a complex and heterogeneous structure across various spatio-temporal scales. The region is known for its large interannual to decadal rainfall variability with, for example, wet 1950s and 1960s, severe droughts in the 1970s and 1980s and a recovery of the rains in recent decades (Sanogo et al. 2015; Nicholson et al. 2018). The latter was associated with an increase in fluvial floods, particularly in the Sahel region (e.g., Elagib et al. 2021; Massazza et al. 2021). In most West African countries, floods are the most frequent, costliest and deadliest natural hazard (Cullmann et al. 2020). The increase in daily and sub-daily rainfall intensities (Panthou et al. 2014, 2018; Chagnaud et al. 2022) and ensuing flooding intensities is only part of the reason.

Although not the primary cause, the high exposure and vulnerability of the population are another significant factor contributing to the high flood risk and recent disasters observed in West Africa (Di Baldassarre et al. 2010; Dos Santos et al. 2019). In terms of the hazard, future projections indicate that rainfall intensity and the frequency of extreme pluvial and fluvial events are likely to increase, posing substantial socio-economic impacts (Han et al. 2019; Kendon et al. 2019; Finney et al. 2020; Onyutha 2020).

As mentioned earlier, research has shown a significant increase in daily and sub-daily rainfall intensities across West Africa since the drought in the 1970s and 1980s. However, limited research has explored the statistics and dynamical causes of intense multi-day rainfall events in West Africa, which often lead to fluvial floods. Consecutive wet days (CWD), defined as the annual maximum number of consecutive days with daily rainfall of at least 1 mm according to the Expert Team on Climate Change Detection and Indices (ETCCDI; Alexander et al. 2019), have significantly increased in recent decades over the Sahel, whereas no trend has been observed at the Guinea Coast (Sanogo et al. 2015). However, while widely used, CWD statistics do not reveal the total volume of rainfall that falls within the wet spells. In their study of the 2007 floods in West Africa, Paeth et al. (2011) found that this rainy season was not extreme in terms of the daily rain events but of 5-day up to 20-day accumulated rainfall totals. Knippertz et al. (2017) describe a 6-day wet spell over large parts of West Africa at the end of July 2016 during the DACCIWA (Dynamics–Aerosol–Chemistry–Cloud Interactions in West Africa) campaign that was associated with a relatively slow-moving northern (13° N) cyclonic and southern (5° N) anticyclonic vortex with westerly wind anomaly in-between, creating conditions for a wet period. In a recent study by Vondou et al. (2025) such slow-moving vortices over the Gulf of Guinea and southern West Africa have been associated with late season wet spells over the Cameroon Line Mountains in October 2019 that were related to the occurrence of a deadly landslide.

However, studying intense rainfall events requires robust statistical documentation from a dense network and long-term in situ rainfall data. Limited access to reliable station data has forced many researchers to use reanalysis (Gbode et al. 2022), satellite (Crétat et al. 2014) and climate model (Sylla et al. 2013) datasets, which often have biases and uncertainties (Maranan et al. 2020; Gosset et al. 2018; Casse et al. 2015; Roca et al. 2010). The accuracy of these data depends on the spatio-temporal patterns and the number of gauging stations used (Schamm et al. 2014). Climate models' difficulties in representing complex regional rainfall patterns further limit their reliability (Biasutti 2013; Monerie et al. 2020; Afiesimama et al. 2006). Quality in situ measurements remain the most reliable for studying intense rainfall characteristics. This study aims to document and characterise intense wet spells over multi-day timescales with respect to frequency, intensity and size. These were achieved using a unique set of consistent long-term daily rainfall data from 239 gauging stations taken from the extensive Karlsruhe African Surface Station data base (KASS-D, Vogel et al. 2018). Additionally, datasets from the Global Precipitation Climatology Center (GPCC; Becker et al. 2013; Schamm et al. 2014), Climate Hazards Group Infrared Precipitation with Stations (CHIRPS; Funk 2015) and Integrated Multi-satellite Retrieval for Global Precipitation Measurement (GPM-IMERG V07; Huffman et al. 2020) were used to examine how they capture the characteristics of intense mult-iday wet spells. Thus, this study also focuses on identifying similarities and differences between various precipitation estimates without delving into comparisons, as done by Sanogo et al. (2022) and Gbode et al. (2022).

In the remaining part of this paper, Section 2 describes the study area and in situ, GPCC, CHIRPS and GPM-IMERG datasets used while Section 3 contains a comprehensive explanation of the method used. Results and discussion are presented in Sections 4 and 5 contains summary and conclusion.

2 | Area of Study and Datasets Description

2.1 | Study Area

The study focuses on a larger area of West Africa, covering Nigeria, Benin, Togo, much of Ghana and Burkina Faso and parts of southern Niger (Figure 1) based on the availability of station data in KASS-D. The region's topography ranges from coastal lowlands to over 2000 m above sea level at the Cameroon Line Mountains, reaching more than 4000 m at the volcano of Mount Cameroon, influencing rainfall distribution (Omotosho and Abiodun 2007). West Africa is divided into Guinea Coast (4°–8° N), Savannah (8°–11° N; often termed the Soudanian zone) and Sahel (11°–16° N) based on ecosystems, climate and land use/land-cover (Omotosho and Abiodun 2007). This classification provides a scientifically established framework that captures the major ecological and climatic gradients across West Africa, thereby allowing a more meaningful comparison of rainfall characteristics and trends among the distinct climatic zones. Rainfall is affected by the Inter-Tropical Discontinuity (ITD), which shifts from 22° N in August to 6° N in January/February (Nicholson 2013). From May to October, the Guinea Coast experiences bimodal rainfall with a little dry season in August, while the Savannah and Sahel have a unimodal pattern peaking in August. Annual rainfall ranges from 1200 to 1500 mm at the Guinea Coast, dropping to less than 900 mm in the Sahel (Diallo et al. 2016). Variability in rainfall can impact the region's economy and agriculture, making this study crucial for climate change risk management (Sultan et al. 2019).

2.2 | Rain Gauge Data and Quality Control Within KASS-D

Despite advancements in satellite rainfall estimation, these products suffer from biases, especially for extreme rainfall events (Ageet et al. 2022). Thus, whenever available, direct station measurements are preferred. In West Africa, meteorological station networks are sparse, and many stations are not included in the Global Telecommunication System (GTS). To largely overcome the data paucity, daily rainfall data from KASS-D (Ageet et al. 2022; Vogel et al. 2018) were used for this study, providing consistent long-term daily rainfall data from 239 stations with at least 80% data coverage from 1982 to 2020. This period includes the droughts of the 1980s and the wetter decades of the 1990s and 2000s. Figure 1 shows the station distribution.

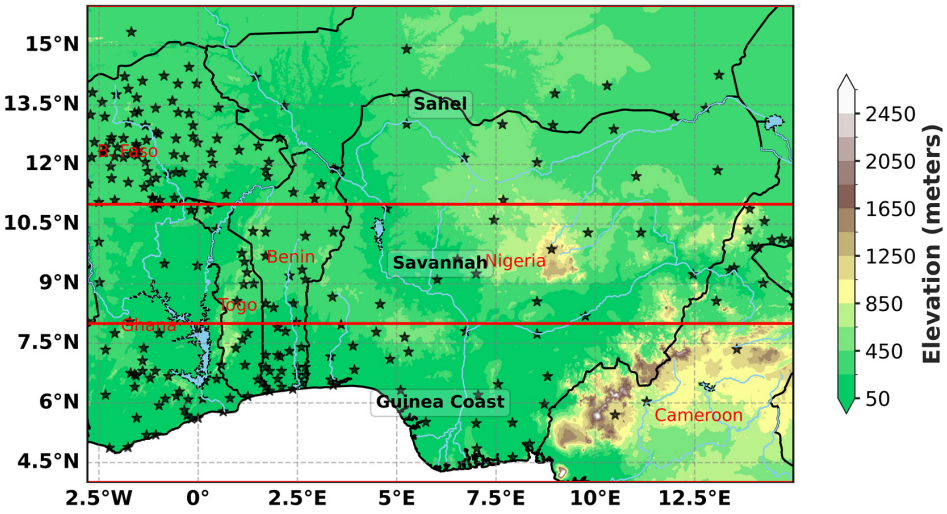

FIGURE 1 | The study area with location of the rain gauge stations used for Spheremap interpolation (red stars) and the climatic zones of Guinea Coast (4°–8° N), Savannah (8°–11° N) and Sahel (11°–16° N) based on Omotosho and Abiodun (2007). The colour shading shows the elevation from Global Land One-km Base Elevation Project (GLOBE; Hastings et al. 1999). [Colour figure can be viewed at wileyonlinelibrary.com]

Rainfall's high spatial and temporal variability complicates automated quality control. Fiebrich and Crawford (2001) established a global range (0–1825 mm) for 1-day accumulated precipitation, which all the selected KASS-D data satisfied. Thereafter, we used two quality control steps: timestamp consistency (Beck et al. 2017) and outlier detection through techniques like 'letter-value plot' analysis and accumulation curves. All the 239 stations with over 80% data availability used in this study passed this quality control check.

2.3 | Gridded Rainfall Products

To enhance the analysis of intense rainfall events over West Africa, three additional gridded rainfall products were used with KASS-D: Global Precipitation Climatology Center (GPCC) version 2022 at 1° resolution (Schamm et al. 2014; Becker et al. 2013), Climate Hazards Group InfraRed Precipitation with Station data version 2 (CHIRPS v2; Funk 2015) at 0.25° resolution, and Integrated Multi-satellite Retrieval for Global Precipitation Measurement (IMERG) version 07 (Huffman et al. 2020) at 0.1° resolution. GPCC provides global daily rainfall data at 1° resolution from January 1982 to near-real-time, based on various gauge observations interpolated using a modified SPHEREMAP method (Becker et al. 2013; Schamm et al. 2014). Figure 2a shows the maximum number of KASS-D rainfall gauging stations in a 1° grid cell for 2020, compared to GPCC (Figure 2b). KASS-D has more consistent and stable measurements than GPCC (Figure 2c), although a significant decrease in gauging stations around 2014 (KASS-D) underscores the challenges of accessing in situ data in West Africa. Despite this, KASS-D is taken as a reference in this study for reasons of representing direct ground-based measurements ('ground truth') from a superior sample of stations compared to GPCC.

In addition to gridded station-based data, the gridded satellite-based products CHIRPS and IMERG are used. According to Funk (2015), CHIRPS provides rainfall estimates globally on daily, five-day and monthly scales, using global precipitation climatology (CHPclim), thermal infrared (TIR), cold cloud duration (CCD) and rain gauge (RG) data. TIR-CCD data, calibrated with TMPA 3B42, are combined with CHPclim to generate Climate Hazard Infrared Precipitation (CHIRP), which is then merged with RG data to produce CHIRPS at five-day and monthly intervals. CHIRPS five-day estimates are further disaggregated into daily amounts using CCD data. IMERG offers global precipitation rate estimates at 0.1° resolution every 30 min, with three processing runs for varying latency needs. The latest version (V07) reprocesses over 20 years of TRMM and GPM data (Huffman et al. 2020). Tan et al. (2022) highlight improvements in V07 over V06, including fixes for high satellite-only estimates, better precipitation distribution with the Kalman filter, orography adjustments, enhanced infrared algorithms, revised phase parametrization and climatological gauge adjustments.

3 | Methodology

Intense or extreme rainfall events are defined by their frequency, intensity, severity and spatial extent. A preliminary analysis of the ungridded KASS-D rainfall data highlighted the need to interpolate data from 239 stations onto a regular grid. This step is important to accurately represent the spatial coverage of intense multi-day wet spells. This interpolation makes KASS-D comparable to other products used.

3.1 | Interpolation and Regridding Method

After all the rainfall gauging stations selected from the KASS-D database, which exhibited 80% data coverage in the study period, passed the quality control check, they were interpolated to a 1° by 1° regular grid size using SPHEREMAP (Willmott et al. 1985) interpolation method, which GPCC is also based upon. Thus, comparability between the station-based datasets KASS-D and GPCC is ensured. Detailed information can be obtained from Willmott et al. (1985) and Becker et al. (2013).

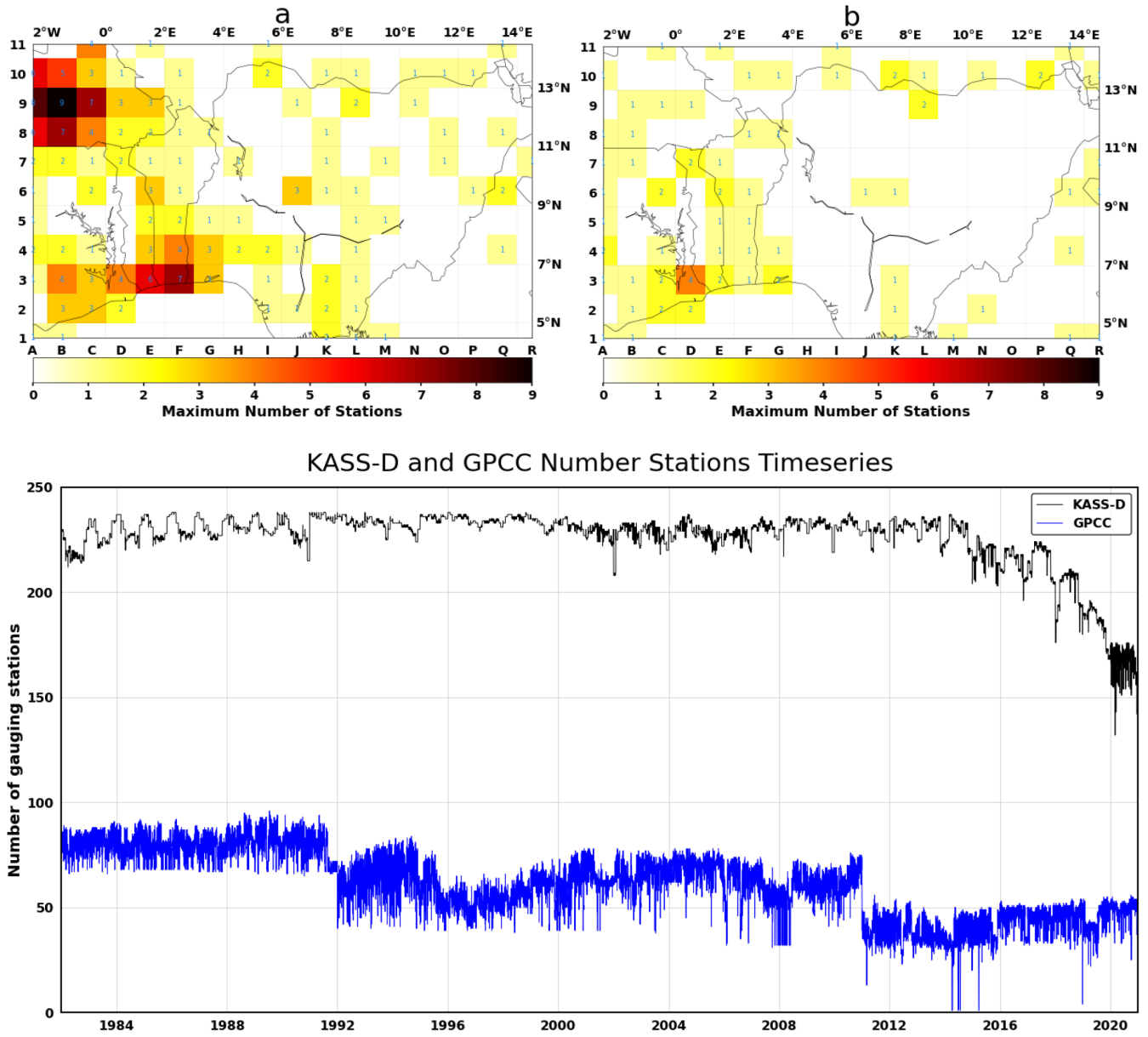

FIGURE 2 | Maximum number of gauging stations per 1° ×1°grid cell with valid observation for the year 2020 for KASS-D (a) compared to GPCC (b). Also shown in (c) is the daily time series of aggregated number of gauging stations per 1° ×1° grid cell over the study area for KASS D (black) and GPCC (blue) from 1982 to 2020. [Colour figure can be viewed at wileyonlinelibrary.com]

This interpolation method has also been used by Nguyen-Xuan et al. (2016) and Thiemig et al. (2021). GPCC modified this interpolation method for regions in the world with dense data coverage but at the same time reverted to the SPHEREMAP method in data-sparse areas, like West Africa.

In the application of the SPHEREMAP interpolation method, the daily rainfall fractions defined as the ratio of daily rainfall to the corresponding monthly total were used instead of the absolute daily values at each station. After the interpolation, the resulting interpolated daily fractions were multiplied by the interpolated monthly totals to derive the final gridded daily rainfall amounts. This procedure is known as Climatology Aided Interpolation (CAI, Willmott and Robeson 1995; Schamm et al. 2014). It has the advantage of adding climatological data to increase the precision of spatial detail while still producing a daily product (Parmentier et al. 2015). In the configuration of the SPHEREMAP used in this study, at a particular grid node, the minimum and maximum number of neighbouring stations required to interpolate station measurements to a regular grid are 4 and 10, respectively. The grid cell size is 1.0° while the grid nodes/points are the same as those of GPCC. We also retained the weighting method used by Willmott et al. (1985) and used the same method described by Shepard (1968) to determine the initial search radius to locate the nearest stations.

The performance of the configuration of SPHEREMAP used with a test dataset provided by GPCC for a year (1988) is satisfactory (see Figures S1 and S2). We remapped CHIRPS and IMERG datasets to a common grid of 1° by 1° to match that of GPCC and KASS-D using the first-order conservative

remapping (Jones 1999) approach (remapcon) of the Climate Data Operators (CDO; Schulzweida 2023). For wet days only with at least a daily rainfall amount of 1.0 mm, we make use of Quantile–Quantile (Q–Q) plots to compare the distribution of wet days in GPCC, CHIRPS and IMERG to KASS-D at selected pixels based on the number of stations within KASS-D grid cells by using the combination of axes alphabet and number labeling in Figure 2a.

3.2 | Intense Multi-Day Wet Spell Definition and Identification

A wet spell is a consecutive period of days with daily rainfall greater than or equal to a threshold. In this study, we define wet days as having at least 1.0 mm of rainfall and focus on intense 3-day and 5-day events for each grid cell because 3–8 days wet spells are dominant over West Africa (Froidurot and Diedhiou 2017; Ratan and Venugopal 2013). This daily rainfall threshold was chosen to conform to the threshold used to define wet days in ETCCDI extreme indices calculation (Alexander et al. 2019; Froidurot and Diedhiou 2017). To identify these intense events, we apply the following conditions:

i. 3-day intense events: A 3-day rolling accumulation with at least two wet days.
ii. 5-day intense events: A 5-day rolling accumulation with at least three wet days and no consecutive two dry days.

A major reason for allowing a dry day within a sequence of wet days in the wet spell definition is grounded by the fact that daily rainfall over West Africa exhibits the lowest level of persistence in the world (Roehrig et al. 2013). West and Central Africa are virtually the only areas worldwide where the auto-correlation of rainfall at a 1-day lag is negative (see Fig. 16 of Roehrig et al. 2013). Hence, the probability of a wet day following a previous wet day is considerably diminished compared to other regions on earth. We computed a spatially varying threshold of the 90th percentile rainfall amount for 3-day and 5-day periods from 1982 to 2020 (KASS-D, GPCC, CHIRPS) and 2001 to 2020 (IMERG; because of its shorter period of availability). Intense wet spells are defined as days when the accumulation exceeds the 90th percentile values for 3-day and 5-day periods at each grid point in each dataset. The last day of the wet spell is used as the timestamp. Froidurot and Diedhiou (2017) evaluate 2–3 day wet spells, which is in line with our definition of a 3-day wet spell of at least 2 wet days.

3.3 | Intense Multi-Day Wet Spell Characteristics and Trend Analysis

We focused on the frequency, intensity and spatial coverage of intense multi-day wet spells. For frequency, we counted the number of events per month when 3-day and 5-day accumulation amounts exceed their 90th percentile at each 1° ×1° grid point, averaging these counts over the Guinea Coast (4°–8° N), Savannah (8°–11° N) and Sahel (11°–16° N) to provide a seasonal representation (Roxy et al. 2017; Ratan and Venugopal 2013). Monthly counts of intense spells were aggregated into annual totals. The spatial coverage (size) of intense events was assessed by counting grid cells exceeding the threshold in a given event and classifying them as small (1–9 cells; approximately ~124,00–111,600 km^2), mid-size (10–20 cells; ~124,000–248,000 km^2), or large (> 20 cells, > 248,000 km^2). The intensity of the intense wet spells used to examine its contribution to annual rainfall amount was quantified as exceedance rainfall amount which indicates the difference between the actual 3- and 5-day wet spell rainfall accumulation and the 90th percentile value of the 3- and 5-day event. The average size (in gridcells) of intense 3-day and 5-day events in a year was then computed using Equation (1);

$$\text{Average size} = \frac{T_{gc}}{\text{Total Number of Events in a Year}} \quad (1)$$

where T_{gc} is the annual aggregate of the number of grid cells per event having a 3-day/5-day accumulation amount greater than 90th percentile value. In addition, the annual maximum size of intense 3-day and 5-day events that occurred in each year was also identified and analysed.

Frequency, average and maximum size and various sizes of 3-day and 5-day intense wet spells were analysed for trends using the modified Mann–Kendall test at a 95% confidence level (Yue and Wang 2004). The Yue and Wang (2004) variant of modified Mann–Kendall test improves upon the traditional Mann–Kendall test (Kendall 1975) by accounting for autocorrelation (serial correlation) commonly present in environmental and climate time series. While the original Mann–Kendall test assumes that observations are independent, this assumption is often violated in climate data, leading to inflated significance and false trend detection. The Yue and Wang variant chosen corrects the test statistic's variance to reflect the effective sample size, while ensuring more reliable and accurate trend detection in autocorrelated datasets like rainfall or temperature extremes.

4 | Results and Discussion

While we present the results of our analysis in this section, it is important to state that due to the shorter period of IMERG rainfall data (2001–2020) compared to other datasets (1982–2020), we exclude IMERG from all the temporal and trend analyses.

4.1 | Comparison of Daily Rainfall Values Between Station- and Satellite Products

As described in the methodology section (Section 3), we define a wet day as any day with at least 1.0 mm of rainfall, and all rainfall products were compared at a daily timescale.

Figure 3 shows Q–Q diagrams comparing daily precipitation values between interpolated KASS-D (*x*-axis) and GPCC (blue curve), IMERG-V7 (green curve) and CHIRPS (red curve) datasets. The Q–Q plots are examples for nine different pixels with varying numbers of stations within the pixel in KASS-D (see Figure 2a). Points above the diagonal line indicate

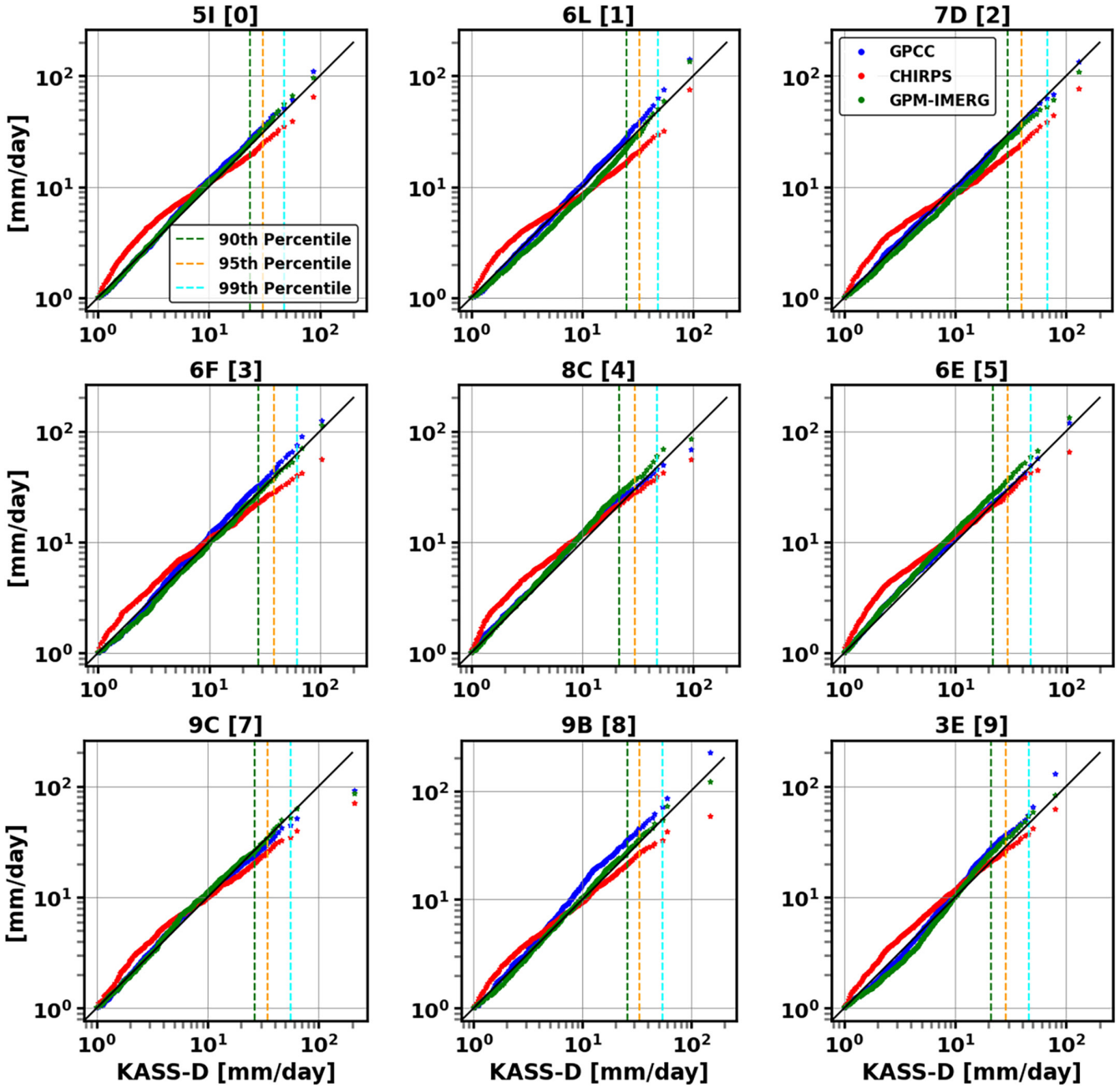

FIGURE 3 | Quantile–Quantile plot of wet days only for selected grid cells using the combination of axes alphabet and number labeling from Figure 2a and based on the number of gauging stations within the 1° ×1° grid cell (number in squared bracket). The *y*-axis corresponds to GPCC, CHIRPS, and IMERG while the *x*-axis corresponds to the KASS-D (reference) dataset using a logarithmic scale that makes the differences appear less dramatic in the upper quantiles than they are. Blue, red and green dots depict GPCC, CHIRPS and IMERG datasets. Vertical green, orange, and cyan broken lines depict KASS-D 90th, 95th and 99th, percentile locations. The black solid diagonal line depicts the ideal fit line (1:1). [Colour figure can be viewed at wileyonlinelibrary.com]

overestimation, while points below indicate underestimation compared to KASS-D. CHIRPS consistently overestimates lower quantile values and underestimates upper quantile values. GPCC generally has higher values in the upper quantiles and is in close agreement with KASS-D in the lower quantiles. However, in grid cell '5I[0]' without gauging stations, GPCC and IMERG show similar distributions close to KASS-D because IMERG is calibrated with GPCC. In the upper quantile, IMERG's higher quantile values are closer to those of KASS-D but less than GPCC's values in most pixels.

To further verify SPHEREMAP configuration used, Figure 4 compares wet days' rainfall amounts from interpolated KASS-D to the arithmetic mean of stations within the same pixel using Q–Q plots, except for pixel '5I' (without stations) replaced by pixel '3F'. In pixels with 1–4 gauging stations, the arithmetic mean closely aligns with the ideal line, indicating values close to KASS-D. Underestimation occurred in pixels with more than four stations compared to KASS-D, likely due to SPHEREMAP weighting method, influence of neighbouring stations and stations with extremely low values, resulting in lower quantiles.

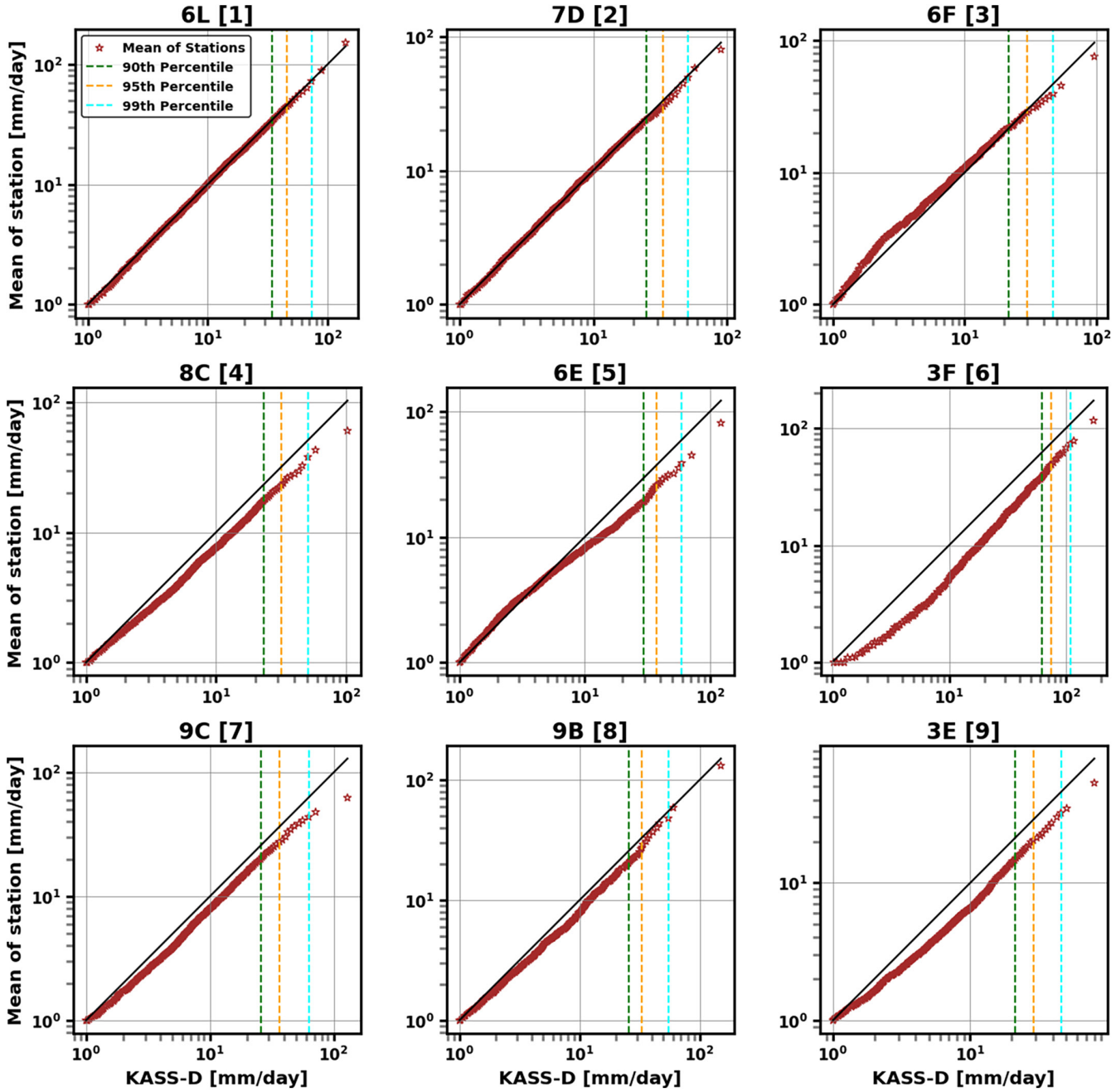

FIGURE 4 | Quantile–Quantile plot of wet days only for selected grid cells and a number of gauging stations within the 1° × 1° grid cell (number in squared bracket). The *y*-axis corresponds to the arithmetic mean of stations within the selected grid cells while the *x*-axis corresponds to the KASS-D (reference) dataset using a logarithmic scale that makes the differences appear less dramatic in the upper quantiles than they are. Vertical green, orange, and cyan broken lines depict KASS-D 90th, 95th and 99th, percentile locations. The black solid diagonal line depicts the ideal fit line (1:1). [Colour figure can be viewed at wileyonlinelibrary.com]

SPHEREMAP performs similarly to the arithmetic mean in pixels with fewer stations. Similar comparisons of GPCC, CHIRPS and IMERG to interpolated observation data have been reported by Ageet et al. (2022) and Sanogo et al. (2022), who noted underestimation and overestimation of upper and lower quantile values, respectively, by CHIRPS in different parts of Africa.

The differences in the wet days' rainfall amount between KASS-D, GPCC and the arithmetic of stations can be linked to the difference in the number of gauging stations per pixel used during interpolation, the percentage of available data, different quality control (QC) methods, the distance of each gauging station to the grid nodes that determined their weight and/or the search radius used. Also, CHIRPS and IMERG are gauge-satellite blended datasets, whereas KASS-D and GPCC are gauge only.

4.2 | Climatological 3-Day and 5-Day 90th Percentile Value and Frequency of Occurrence

The spatial distribution of the 90th percentile value for 3-day and 5-day accumulation rainfall amounts is shown in

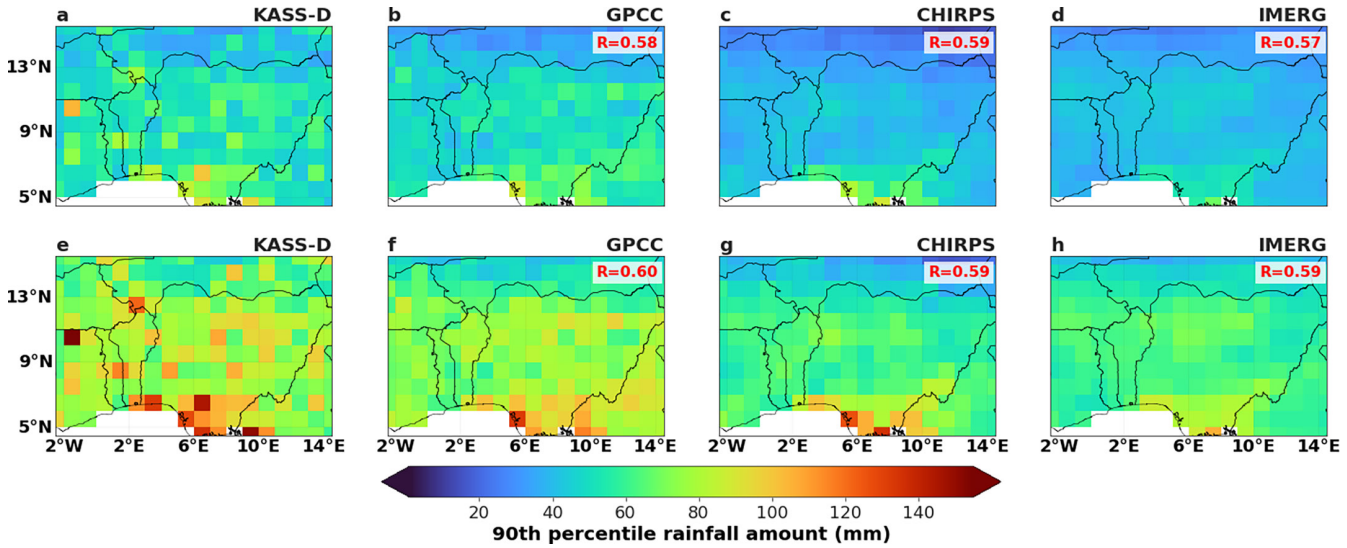

FIGURE 5 | Spatial distribution of 90th percentile 3-day (first row) and 5-day (second row) accumulation rainfall amount over the domain. KASS-D, GPCC, and CHIRPS 90th percentile values are computed from 1982 through 2020 while IMERG is from 2001 to 2020. Red colour value at the upper right corner shows the spatial correlation coefficient between KASS-D 90th percentile accumulation amount and other rainfall products. [Colour figure can be viewed at wileyonlinelibrary.com]

Figure 5 for each dataset from 1982 through 2020 (KASS-D, GPCC and CHIRPS) and 2001–2020 (IMERG). Also, Figure S3 depicts the difference in 90th percentile values between other rainfall products and KASS-D. This difference between GPCC and KASS-D is lower, especially over Nigeria, Burkina Faso and Cameroon mountain compared to CHIRPS and IMERG. The 90th percentile values for the 3-day and 5-day accumulation display a largely meridional variation over the domain in all the datasets, with the coastal and Niger Delta regions of Nigeria having the highest 90th percentile accumulation values.

For KASS-D, the 3-day and 5-day 90th percentile have a maximum value of 90 and 140 mm, respectively, that extends from the coastal region of Nigeria to the Cameroon highland area that then decreases to the far north (Figure 5). The latitudinal variation of 3-day and 5-day 90th percentile amounts in KASS-D can be seen in all other datasets irrespective of the data period. In the inland area, the 3- and 5-day 90th percentile amounts depicted by KASS-D and GPCC are higher than the amount shown by satellite products. This is similar to the spatial variation of mean annual rainfall over West Africa that is defined by the north and south oscillation of the rainbelt (Nicholson 2013). However, the latitudinal variation in satellite-based products (CHIRPS and IMERG) is smoother and relatively low compared to rain gauge-based products (KASS-D and GPCC). The spatial correlation coefficients between the 90th percentile of 3-day accumulated rainfall from KASS-D and other rainfall products range from 0.57 to 0.59, while those for 5-day accumulations fall between 0.59 and 0.60. This artefact can be associated with the algorithm adopted by these satellite-based datasets that estimate daily rainfall amount at equal distances (grid points) using different means like TIR-CCD (Kidd and Levizzani 2011). In addition, this can also be attributed to long and smooth decorrelation lengths in CHIRPS or PMW-based approaches in IMERG compared to direct rainfall measurements by rain gauge that are not equidistant from each other.

Using the 90th percentile value of 3-day and 5-day accumulation amounts at each grid point as a threshold, an intense multi-day wet spell occurred when accumulation rainfall for each duration exceeds their respective threshold on a given date. Counting the number of intense multi-day wet spell events in each year, Figure 6 depicts the spatial distribution of the annual mean number of intense 3- and 5-day wet spells and the mean annual number of wet days. Climatologically, the spatial distribution of 3-day intense wet spell frequency of occurrence follows the spatial pattern of the 90th percentile value in Figure 5. KASS-D annual mean frequency of occurrence of 3-day intense wet spell in Figure 6a ranges between 13 and 20 over the coastal region and Niger Delta area of Nigeria to events less than 5 events per year north of 11° N. Compared to its surroundings, the mean annual number of intense 3-day wet spells is low over the Ghana-Benin dry zone (aka the Dahomey GapA) due to the observed relative dryness of the area resulting from the combination of frictional divergence oriented along SW–NE coastlines and coastal upwelling of cold waters (Nicholson 2011; Vollmert and Fink 2003).

However, the frequency of occurrence varies from one grid cell to the other between 7.5° N and 11° N in the range of 5 to 12 events per year. All these features are also observed in GPCC, CHIRPS and IMERG but with a slight variation in the mean annual number and spatial pattern of the 3-day intense wet spell. Additionally, differences in rainfall representation over mountain and coastal areas range, particularly the Jos Plateau and the Niger Delta region, between station- and satellite-based products become evident due to the number of stations in the area. The spatial correlation coefficients between the mean annual frequency of intense wet spells derived from KASS-D and those from other rainfall products range from 0.74 to 0.87, while correlations for 5-day precipitation totals lie between 0.76 and 0.88. Among the datasets, GPCC exhibits the strongest agreement with KASS-D, whereas CHIRPS demonstrates the weakest correlation coefficient. This highlights the importance of high

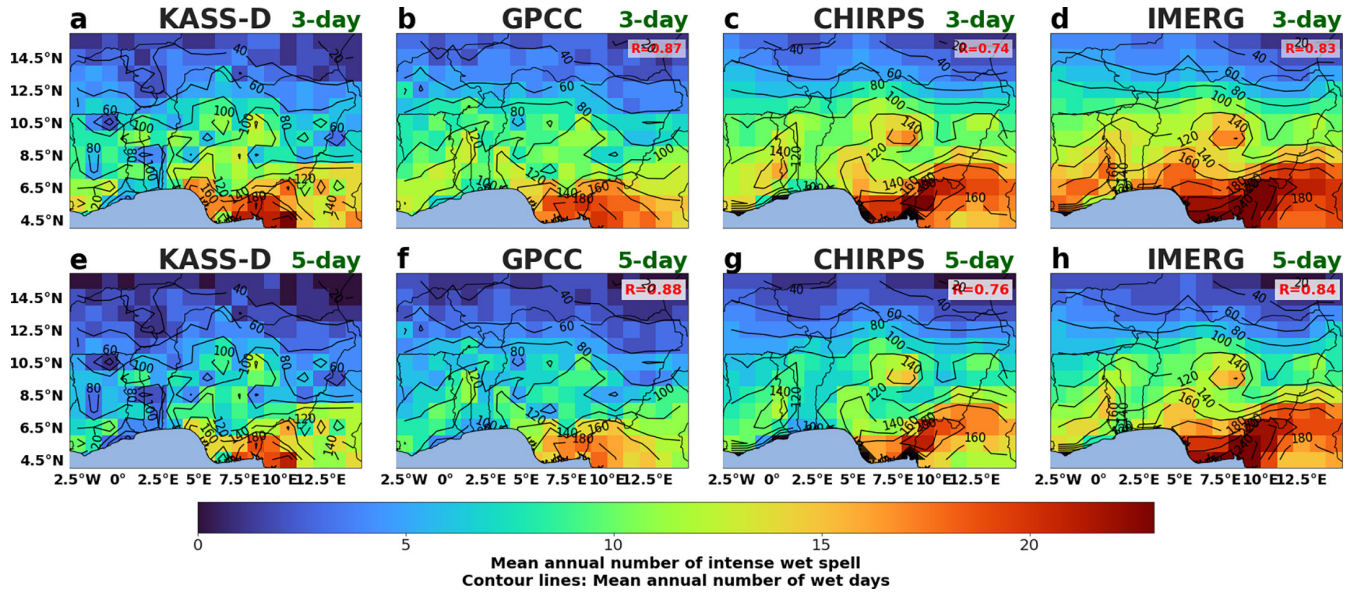

FIGURE 6 | Spatial distribution of mean annual frequency of occurrence of intense 3-day (first row) and 5-day (second row) wet spells (colour fill) and mean annual number of wet days (contour line) from 1982 to 2020 (KASS-D, GPCC, and CHIRPS) and 2001–2020 (IMERG). Red colour value at the upper right corner shows the spatial correlation coefficient between mean annual number of intense wet spells by KASS-D and other rainfall products. [Colour figure can be viewed at wileyonlinelibrary.com]

station density for accurately representing rainfall spatially, which is a significant challenge in West Africa. The mean annual number of wet days (daily rainfall amount greater than 1 mm) decreases from the coastal region to the far north. At the Coast and Niger Delta in particular, KASS-D and GPCC have an average number of about 180 wet days (contour lines) in a year but lower than satellite-based datasets (CHIRPS and IMERG) average number of wet days. The mean annual number of wet days decreases with an increase in latitude to less than 40 days in the far north (north of 14° N). Similarly, the spatial distribution of the occurrence of 5-day intense wet spells is highly similar to 3-day but lower in magnitude.

4.3 | Seasonal and Annual Variation of 3-Day and 5-Day Wet Spells

Figure 7 illustrates the seasonal variability of 3- and 5-day intense wet spells across the Guinea Coast, Savannah and Sahel. In all months and zones, 3-day wet spells occur more frequently than 5-day wet spells. The Guinea Coast shows smaller differences between 3-day and 5-day spells compared to the Savannah and Sahel, likely due to fewer rainy days in the latter regions and the Guinea Coast's proximity to the Atlantic Ocean and frequent convective activities. Over the Guinea Coast, the number of 3-day and 5-day intense wet spells exhibits a bimodal pattern, peaking in June and September with fewer than 15 (KASS-D) and 12 (GPCC) events per grid cell in these months. The first peak in June is higher in satellite-based CHIRPS data than the second peak in September, a pattern also observed in IMERG data despite its shorter period. In the Savannah and Sahel, a unimodal pattern appears with a peak in August. The Savannah experiences about 19 3-day events per grid cell in August, higher than the Sahel's fewer than 14 events. Most intense 3-day and 5-day wet spells in the Sahel occur from July to September (Figure 7c,f,i,l), driven by Meso-scale Convective Systems (MCSs) and squall lines, which deliver over 90% of its rainfall (Omotosho and Abiodun 2007; Fink and Reiner 2003).

Figure 8 displays the inter-annual variation in the number of 3- and 5-day intense wet spells per grid cell across the study domain. The occurrence of 5-day wet spells is closely linked to 3-day events, indicating that 5-day spells are often extensions of 3-day spells. The mean annual number of intense 3-day (5-day) wet spells over the study domain ranges from 7.5 (5.5) to 9 (7) events across all datasets. The lowest mean annual number is in KASS-D, while the highest is in CHIRPS. From 1982 to 1999 (Figure 8a), KASS-D shows an increasing trend in the annual number of 3-day and 5-day intense wet spells, reaching 10 and 8 events per grid cell, respectively. However, periods like 1992–1993 and 1995–1998 experienced decreases in frequency, with events per grid cell below the long-term means of 7.9 (3-day) and 4.9 (5-day). Post-2001, there was a significant decline in frequency, followed by an increase until 2012, with many events exceeding the long-term mean. The frequency reduced again after 2012 but showed an upward trend towards 2020. GPCC and CHIRPS exhibit similar inter-annual variation patterns (Figure 8a,b), with slight differences in the years when the frequency of 3- and 5-day wet spells remained above average. The highest frequency of 3-day and 5-day events occurred in 2019 (KASS-D), 1999 and 2007 (GPCC) and 1999 (CHIRPS). Despite the differences in rainfall products and with the correlation coefficient higher than 0.60 (see Supporting Information S4), there is a noticeable level of agreement among the datasets in the patterns of increase or decrease in the annual number of intense wet spells.

According to the modified Mann–Kendall test, an increasing trend in the annual frequency of multi-day wet spells shown by KASS-D in Figure 8 is confirmed by a statistically significant rate of 0.07 events per year for 3-day wet spells and 0.06 events per year for 5-day wet spells (see the text on Figure 8). Further

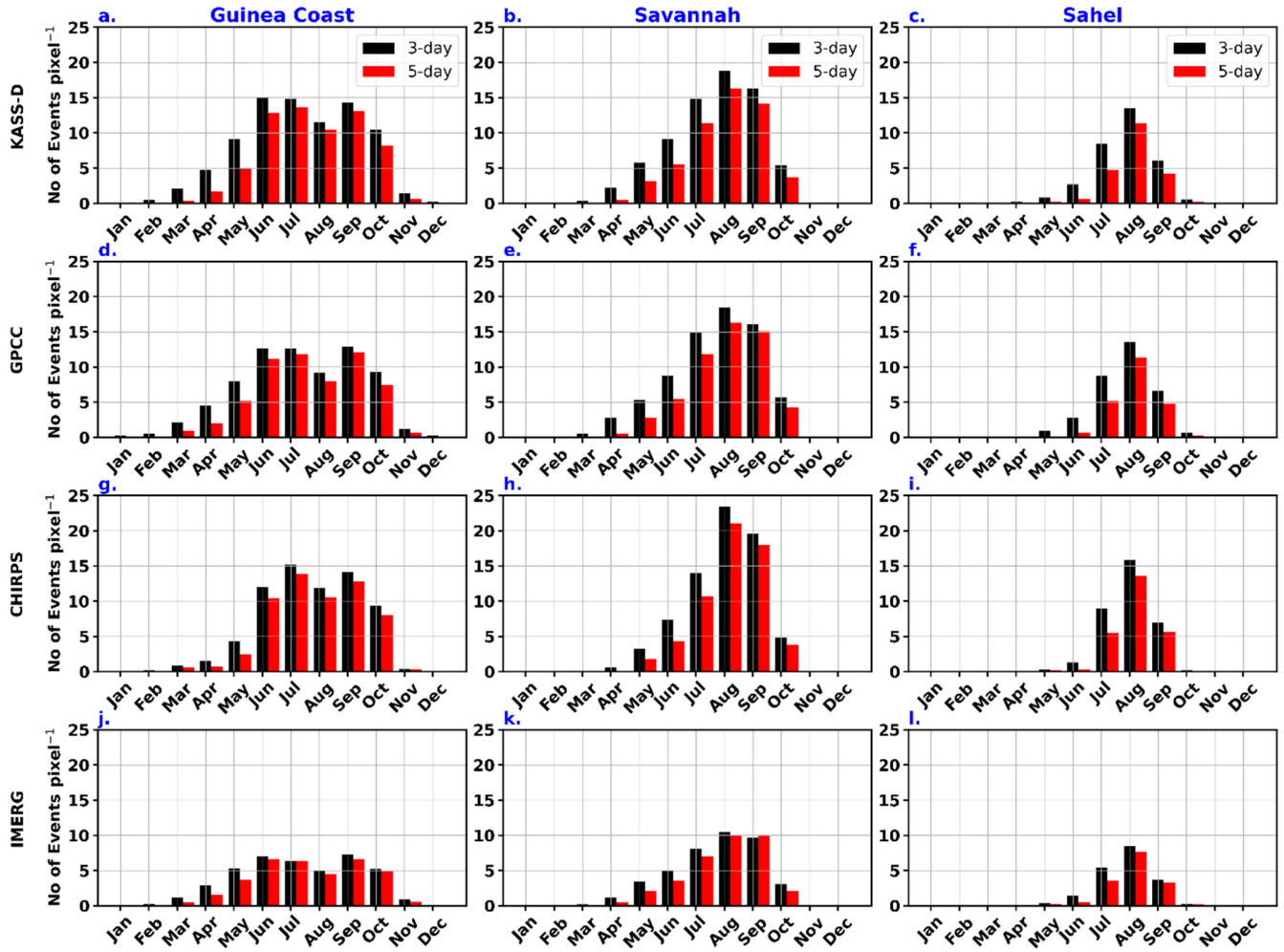

FIGURE 7 | Seasonal frequency of occurrence of intense 3-day and 5-day wet spells per grid cell (pixel) from 1982 to 2020 (KASS-D, GPCC, and CHIRPS) and 2001–2020 (IMERG) averaged over the Guinea Coast, Savannah, and Sahel climatic zones of the study domain. [Colour figure can be viewed at wileyonlinelibrary.com]

modified Mann–Kendall trend tests (not shown) revealed that this increasing trend is largely insensitive to the decreasing trend in the number of KASS-D stations from 2014 onwards (see Figure 2). GPCC showed a statistically significant increasing trend of 0.03 events per year for 3-day only while CHIRPS reported no significant trend for both 3- and 5-day intense events, with trend lines almost parallel to the long-term mean. The significant trend in KASS-D is further explained in Figure 9 by averaging effects of high positive Sen's slope values over Nigeria, Burkina Faso and Niger and low negative values over Ghana, Togo, Benin and the Cameroon Highlands. GPCC and CHIRPS show low positive and high negative Sen's slope values over the same countries compared to KASS-D. This difference is likely due to the higher number of stations in KASS-D compared to GPCC (Figure 2a,b). The increase in the frequency of intense wet spells post-1990 across all datasets may be attributed to the partial recovery of rainfall from the dry years of the 1980s (Sanogo et al. 2015; Nicholson 2013).

The effects of climate change, particularly in the frequency and intensity of extreme weather events, are more pronounced at the local level than globally (IPCC 2021). This study examines the frequency of intense multi-day wet spells across three climatic zones in the domain. The inter-annual variation of 3-day and 5-day intense wet spells per grid cell for KASS-D, GPCC and CHIRPS averaged over Guinea Coast, Savannah and Sahel is shown in Figure 10. At the Guinea Coast (first column in Figure 10), the mean annual occurrence of 3-day wet spells ranges from 11 to 12.5 events per pixel, and 5-day wet spells from 9 to 10 events per pixel across all datasets. The long-term annual mean for 3-day intense wet spells is 11 events/year for KASS-D, 12 for GPCC and 12.5 for CHIRPS. For 5-day intense wet spells, it is 9 events/year for KASS-D, 9.5 for GPCC and 10 for CHIRPS. KASS-D (Figure 10a) shows an increasing pattern of 3-day and 5-day intense events from 1982 to 2020, despite significant lows in the early 1980s and between 2012 and 2018. GPCC and CHIRPS also show an increase from 1982 to 1999, followed by low frequencies from 2000 to 2006 (Figure 10d,g). Both datasets show a decrease towards the end of the study period after sharp increases in 2007 (GPCC) and 2009 (CHIRPS). The low frequency of 3-day and 5-day intense wet spells before 1988 extends to the Savannah and Sahel (Figure 10). The long-term mean frequency of these events in the Savannah and Sahel is lower than in the Guinea Coast, with the Sahel having the lowest. In the Savannah, the first peak of about 10 events/year (KASS-D and GPCC) and more than 16 events/year (CHIRPS)

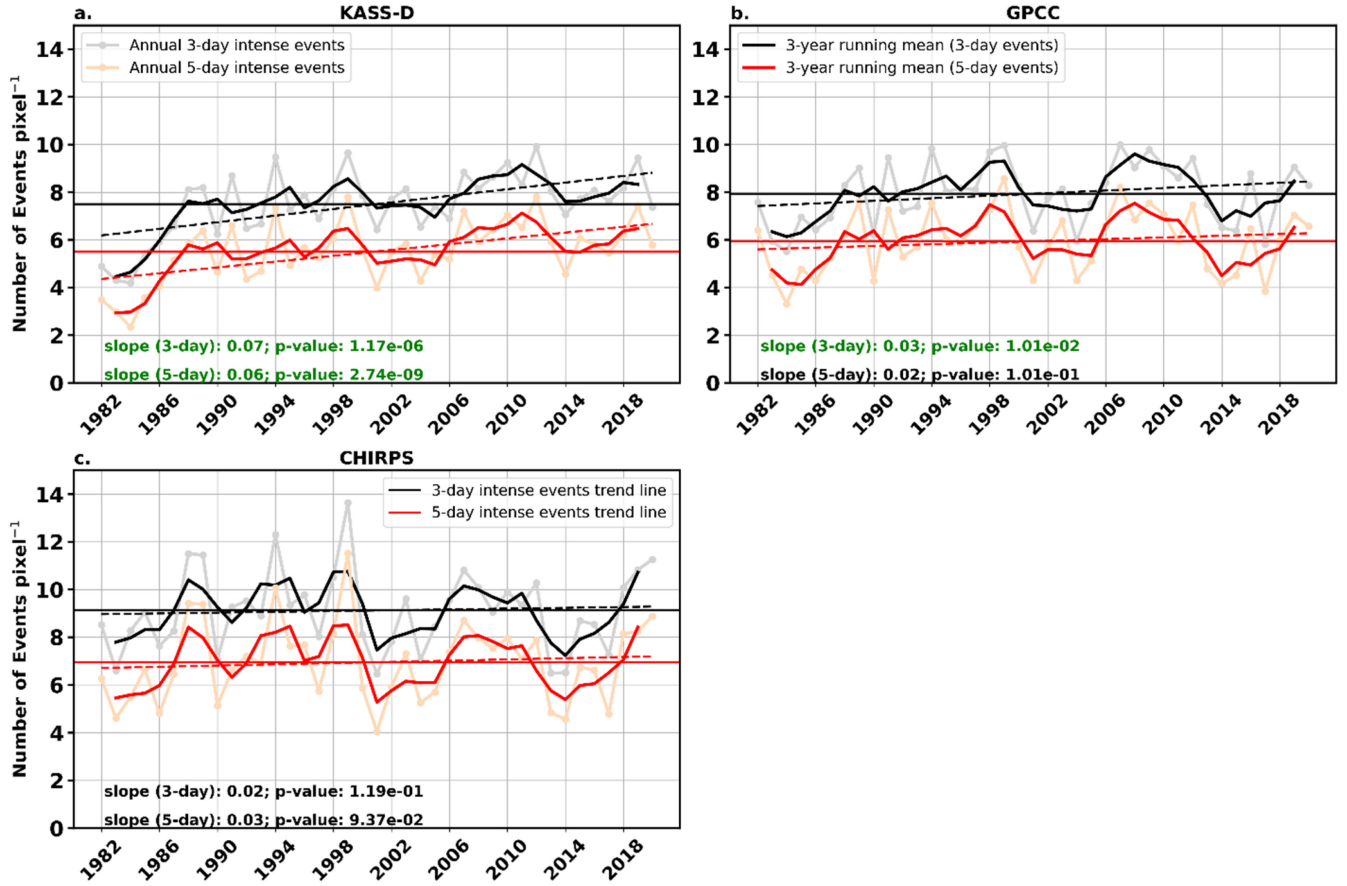

FIGURE 8 | Interannual variations (grey and orange lines with markers) and 3-year running means (black and red lines) of the annual frequency of intense 3-day and 5-day wet spells from 1982 to 2020, averaged over the study domain for KASS-D, GPCC, and CHIRPS datasets. Thin horizontal black and red lines represent the climatological means, while dashed lines of the same colours show the linear trend lines for 3-day and 5-day events, respectively. The Modified Mann–Kendall test results are annotated on each panel, where green (black) text indicates statistically significant (non-significant) increasing trends at 0.05 significance level. [Colour figure can be viewed at wileyonlinelibrary.com]

in 1989 was followed by a significant decrease in 1990 across all datasets. For the Sahel, a higher number of occurrences in 1994 was shown by all datasets, but GPCC and CHIRPS showed reduced numbers from the early 2000s until 2017.

In all datasets, only KASS-D shows consistent upward trends for 3- and 5-day intense wet spells per pixel across all climatic zones, with all datasets agreeing on an upward trend in the Sahel. The level of agreement among the datasets in the patterns of increase or decrease in the annual number of intense wet spells is highest in the Sahel with r higher than 0.87 compared to other zones (Figure S5). The MK t-test (Table 1) confirms this with a significant increasing trend in 3-day/5-day intense wet spells in the Sahel, highest in KASS-D (0.094/0.063) and lowest in GPCC (0.054/0.042). Only KASS-D revealed a statistically significant increasing trend across all the climatic zones, while all the datasets revealed the same statistically significant increasing trend in the Sahale (Table 1).

4.4 | Size Classification of Intense 3-Day and 5-Day Events

The classification of 3-day and 5-day intense wet spells by size, based on contiguous (connected) grid cells exceeding the 90th percentile amount, reveals that small-size events occurred more frequently than mid-size and large-size events at an annual scale (Figure 11). Small-size events decreased between 1982 and 1990, with CHIRPS showing the lowest and KASS-D the highest occurrences, followed by a brief increase in these events before a general decrease. From 1982 to 2020, mid-size events increased overall (Figure 11b,e), despite declines from 2000 to 2005 and 2010 to 2015. CHIRPS reported the highest number of 5-day mid-size events before 1995. Large-size events showed an early increase, with CHIRPS and GPCC above their long-term mean until 2002, followed by two low-occurrence periods (2000–2005 and 2010–2015). CHIRPS focuses on large-scale events might be due to its design since it relies on TIR-CCD, covering a wider area on average. CHIRPS and GPCC displayed a decreasing trend that is significant in small-size events (Table S1), while KASS-D showed no trend. KASS-D and GPCC alone showed a significantly increasing trend for both mid-size and large-size 3- and 5-day intense wet spells, while CHIRPS revealed a significant increasing trend in large-size intense wet spells under both durations. Compared to KASS-D and as Figure S6, GPCC shows the highest linear correlation coefficient value of 0.69 and 0.82 in mid and large size of 3- and 5-day intense wet spells.

The linear correlation coefficients (Figure S6) indicate marked variability in the level of agreement between KASS-D and other

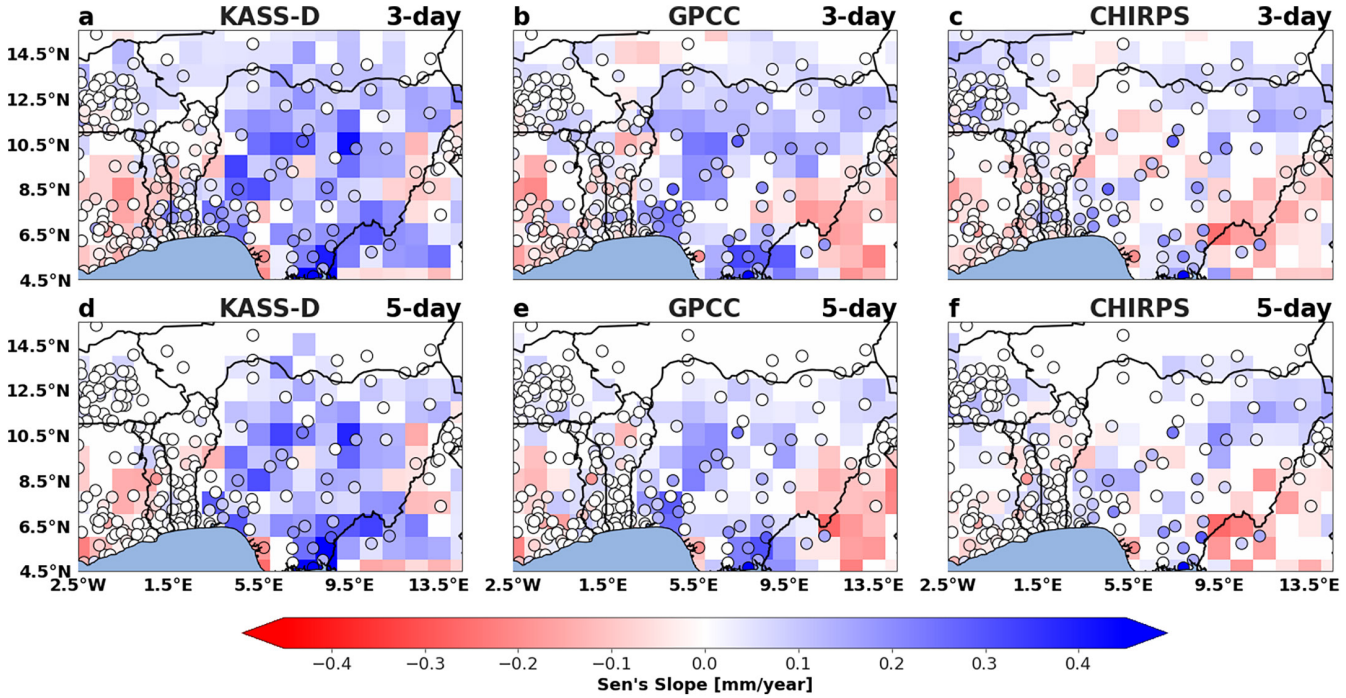

FIGURE 9 | Spatial distribution of Sen's slope value (colour fill) at each grid cell for KASS-D, GPCC, and CHIRPS as indicated on the plot for 3-day (a–c) and 5-day (d–e). Filled scatter plots on each plot represent Sen's slope values computed for each station used in the interpolation of KASS-D. [Colour figure can be viewed at wileyonlinelibrary.com]

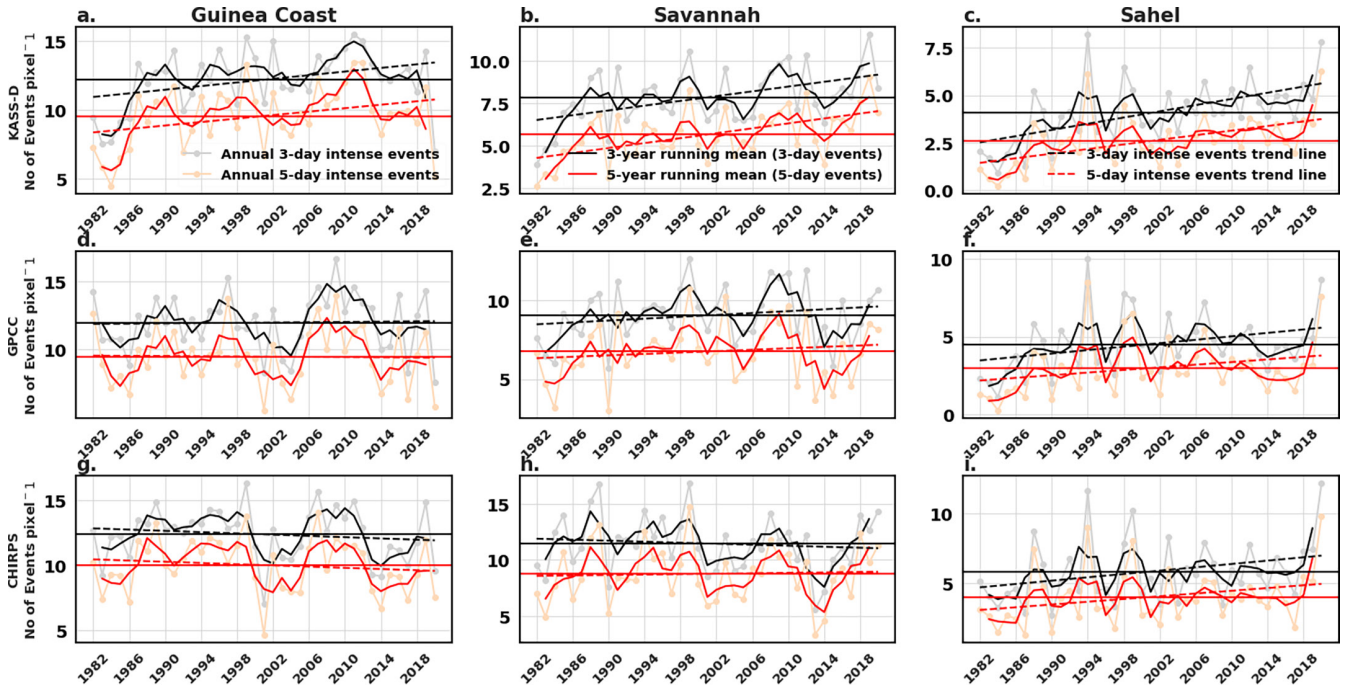

FIGURE 10 | Interannual variations (grey and orange lines with markers) and 3-year running means (black and red lines) of the annual frequency of intense 3-day and 5-day wet spells from 1982 to 2020 averaged over Guinea Coast (first column), Savannah (second column), and Sahel (third column) for KASS-D, GPCC, and CHIRPS datasets. Thin horizontal black and red lines represent the climatological means, while dashed lines of the same colours show the linear trend lines for 3-day and 5-day events, respectively. [Colour figure can be viewed at wileyonlinelibrary.com]

rainfall products across small, mid- and large-sized intense 3-day and 5-day wet spells. For small-size events, correlations remain weak to moderate ($r = 0.17–0.68$), with notably stronger agreement for 5-day accumulations compared to 3-day. Mid-size events exhibit higher consistency, particularly for 5-day wet spells ($r = 0.85$ between KASS-D and GPCC), while large-size events show the strongest correlations overall, reaching up to 0.82 (3-day) and 0.74 (5-day). These indicate that gauge-based

TABLE 1 | Modified Mann–Kendall trend test result for the frequency of occurrence of 3-day and 5-day intense multi-day wet spells over the three climatic zones in the study domain.

		3-day		5-day	
Dataset	**Region**	**Trend**	**Sen's slope**	**Trend**	**Sen's slope**
KASS-D	Guinea Coast	Increasing[a]	0.080	Increasing[a]	0.069
	Savannah	Increasing[a]	0.089	Increasing[a]	0.088
	Sahel	Increasing[a]	0.094	Increasing[a]	0.063
GPCC	Guinea Coast	No trend	0.020	No trend	0.006
	Savannah	Increasing[a]	0.030	No trend	0.025
	Sahel	Increasing[a]	0.054	Increasing[a]	0.042
CHIRPS	Guinea Coast	No trend	−0.025	No trend	−0.025
	Savannah	No trend	−0.007	No trend	0.026
	Sahel	Increasing[a]	0.062	Increasing[a]	0.051

[a]Indicate statistically significant increasing or decreasing trend at 0.05 significance level.

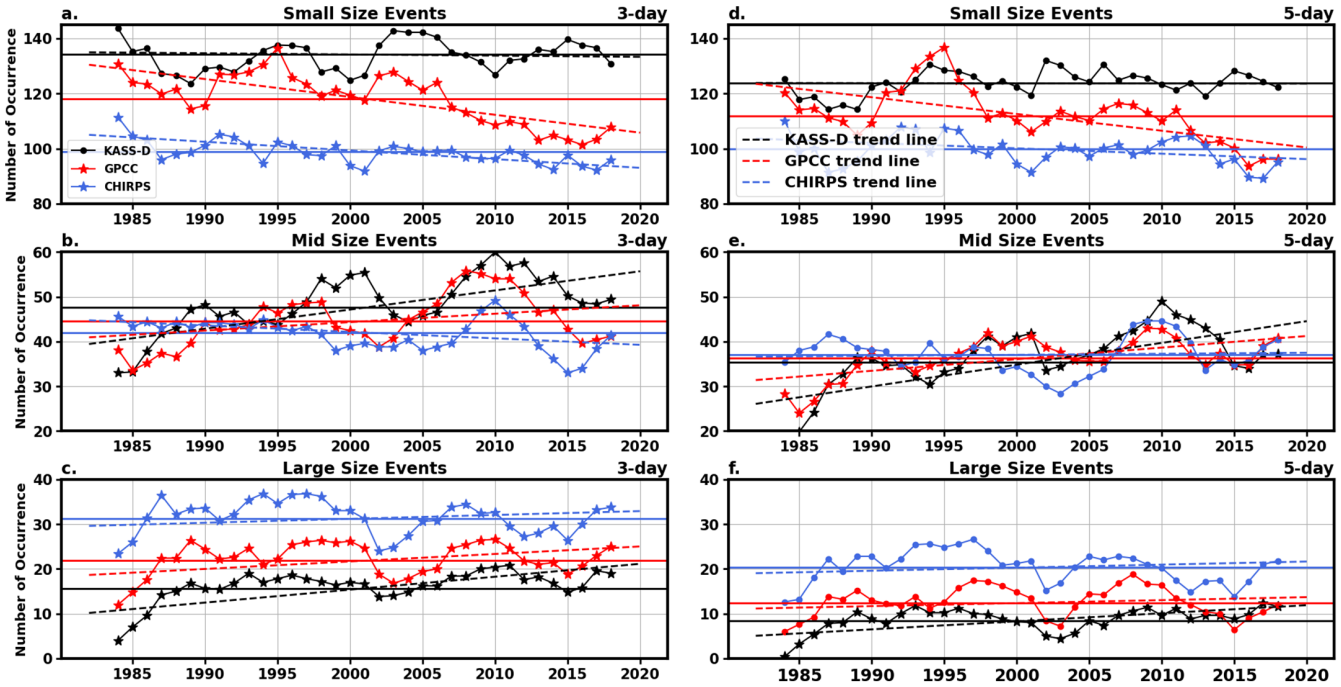

FIGURE 11 | 5-year running mean of an annual mean of small-size (1-9 grid cells), mid-size (10-20 grid cells), and large-size (greater than 20 grid cells) events of 3-day (a–c) and 5-day (d–f) intense wet spells over the domain from 1982 to 2020. Black, red and blue dots marked lines depict KASS-D, GPCC and CHIRPS datasets. Colour thin horizontal lines and dashed lines depict long-term mean and trend lines, respectively. Star marked lines depicts lines where the trend is statistically significant at 0.05 significant level. [Colour figure can be viewed at wileyonlinelibrary.com]

rainfall product (GPCC) more effectively captures prolonged and larger-scale extreme rainfall events, underscoring the critical role of gauge network density in determining the reliability of rainfall products for monitoring extreme rainfall.

4.5 | Average Size and Maximum Size

The average and maximum size of intense events in a year indicate the mean and largest size of all such events within that year. This helps determine whether extreme events are becoming larger and affecting larger areas over time. Figure 12 shows the annual average and maximum size of both 3- and 5-day intense wet spells for all the datasets. The average size of 3-day and 5-day intense wet spells by KASS-D, GPCC and CHIRPS over the years are similar. Long-term average size of 3-day and 5-day intense wet spells by KASS-D is 8.5 and 7 grid cells while GPCC is 9.5 and 8 grid cells and CHIRPS is 11.5 and 10 grid cells, respectively, making CHIRPS have the highest long-term average size among the datasets due to its TIR-CCD information. Before 1990, the average size of 3-day (5-day) intense events increased from 5 (4) grid cells in 1984 to 9 (8) grid

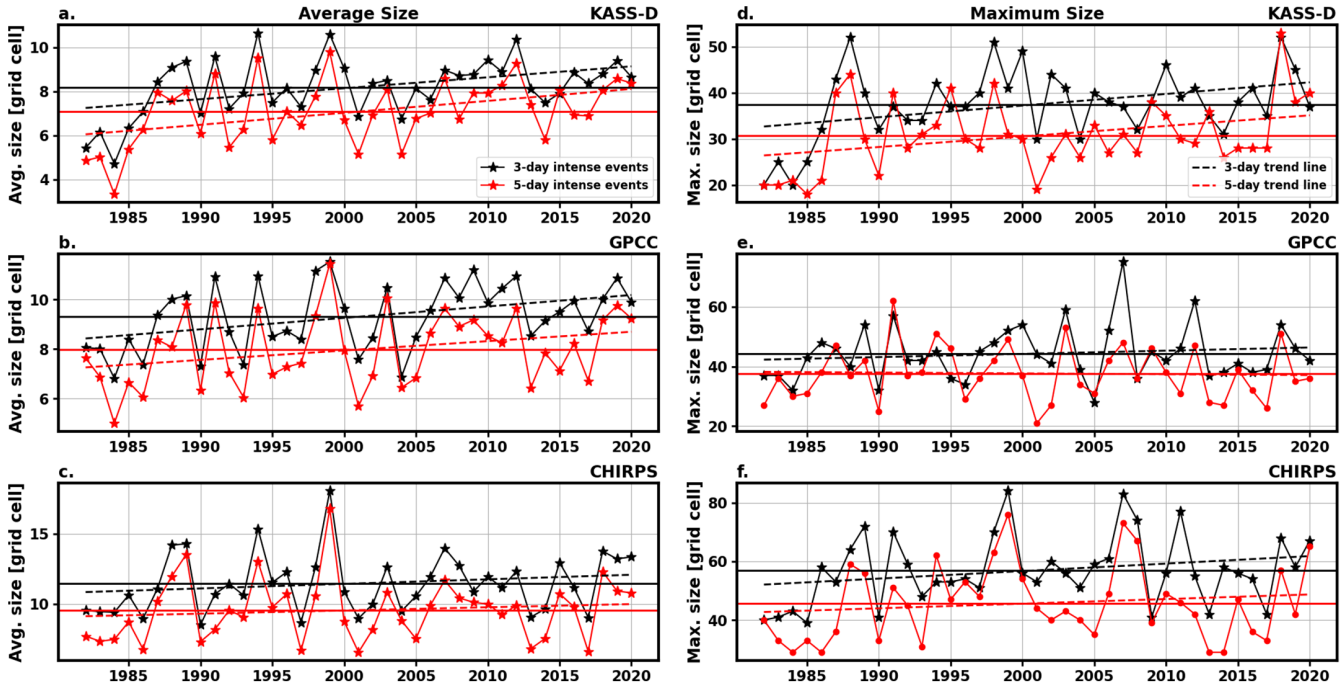

FIGURE 12 | Average and maximum size annual time series of 3-day (left panel) and 5-day (right panel) intense wet spells over the domain. Black and red thick (dashed) lines represent the climatological mean (trend line) of intense 3- and 5-day frequency of occurrence. Star marked lines depicts lines where the trend is statistically significant at 0.05 significant level. [Colour figure can be viewed at wileyonlinelibrary.com]

cells depicted by KASS-D (Figure 12a). From 2004, the average size of both intense events continued to increase in KASS-D until the end of the study period. However, 1991, 1994, 2009 and 2019 are the noticeable years with an average size of both intense events exceeding 9 grid cells. Also, there are periods like 1995–1998 and 2000–2006 (see Figure 12a) when 3-day and 5-day average sizes were observed below the long-term mean despite the increase that occurred in the average size of the intense events over the years. GPCC in Figure 12b shows an upward trend in the average size of intense wet spells similar to what is displayed by KASS-D. With a correlation coefficient equal to or greater than 0.7 (see Figure S7), there is fair agreement among all the datasets regarding the interannual variability of the size of the 3- and 5-day intense wet spells, yielding confidence in the satellite-based product CHIRPS to reliably depict their spatial characteristics in comparison to the station-based products KASS-D and GPCC.

For KASS-D in Figure 12d, the maximum size of 3-day and 5-day intense events increased from 19 and 24 to 53 and 47 grid cells, respectively, between 1982 and 1998, despite the occurrence of years with a decrease in maximum size. After this period, a pronounced decrease in maximum size occurred when the maximum size of 3-day and 5-day wet spells was far below the long-term mean. Comparing this observed pattern to GPCC and CHIRPS (Figure 12e,f), they are similar with differences in the number of grid cells. For example, KASS-D's highest number of grid cells for a maximum size of 3-day and 5-day events occurred in 2019 (Figure 12d) with over 50 grid cells but in GPCC (Figure 12e), it occurred in 2007 with 78 grid cells for 3-day events and 1991 with 62 grid cells for 5-day intense events. This is also true for CHIRPS (Figure 12f) in 1999 and 2007 with a higher number of grid cells. As shown in Tables S2 and S3, all the datasets exhibit a statistically significant increasing trend in the average and size of 3-day and 5-day intense events while that further indicates a significant increase in the spatial extent over these intense events. Similarly, KASS-D, GPCC and CHIPRS showed a robust statistically significant increasing trend in the maximum size of 3-day intense wet spells.

4.6 | Contribution of Intense Wet Spells to Annual Rainfall

Figure 13 displays the 3-year running mean of the percentage contribution of 3- and 5-day intense wet spells to annual rainfall and annual total rainfall amount across the Guinea Coast, Savannah and Sahel. Annual rainfall exhibits marked spatial variability across the three climatic zones, with the Guinea Coast receiving the highest totals and the Sahel the lowest. Notably, in all zones, rainfall during the 1980s remained consistently below the long-term climatological mean, reflecting the persistence of the severe drought episodes that characterised West Africa during this period (Nicholson 2013). The Guinea Coast shows the highest long-term mean proportion of annual rainfall from these intense events, while the Sahel has the lowest. KASS-D indicates an increasing trend in the contribution of intense wet spells across all climatic zones, with the most significant rise in the Sahel (Figure 13a–c). For KASS-D, the contribution of 3-day (5-day) intense wet spells rose from 27% (24%) in the 1980s to 36% (33%) by the end of the study period in the Guinea Coast (Figure 13a). Over the Savannah, the contribution increased from 22% (16%) to 38% (30%) (Figure 13b), and in the Sahel, it rose from 15% (6%) to around 35% (26%) (Figure 13c). GPCC and CHIRPS reveal a less visible increase in the contribution to annual rainfall over Guinea Coast and Savannah, while GPCC reflects a similar increase in the Sahel from 15% (8%) to about 30% (24%)

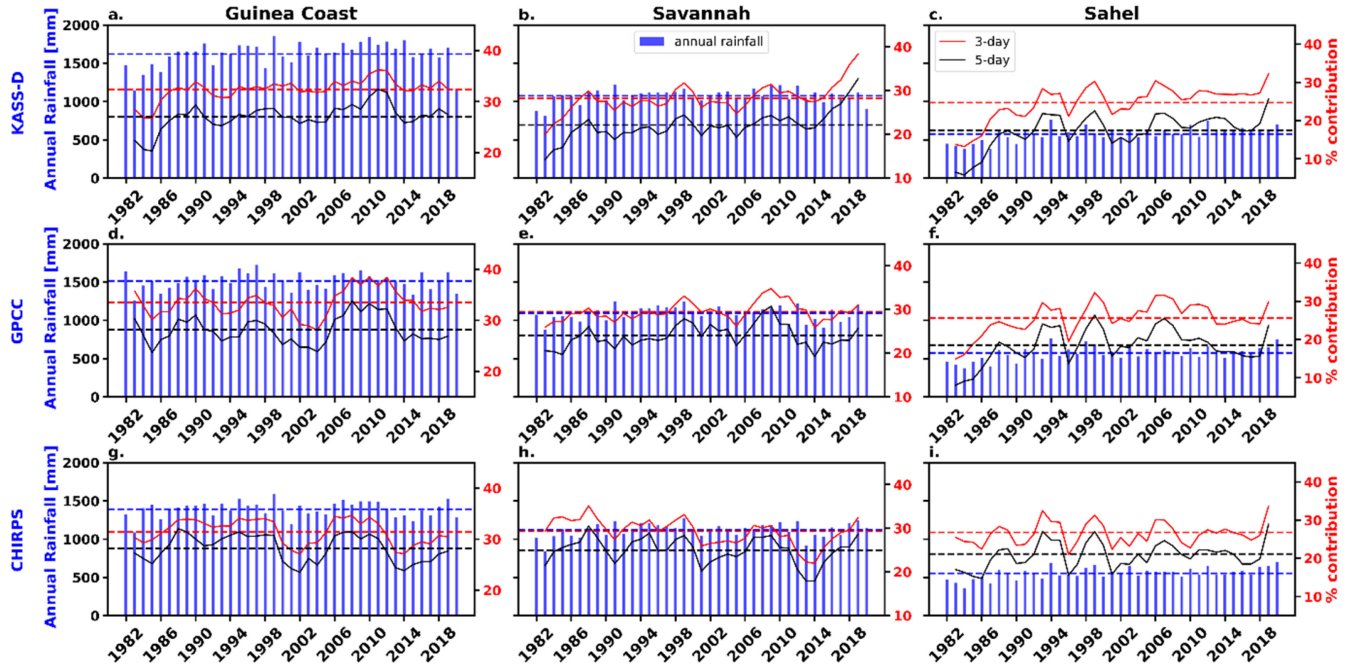

FIGURE 13 | The 3-year running mean of the percentage contribution of 3- and 5-day intense wet spells to annual rainfall amount (right axis) and total annual rainfall (left axis) over Guinea Coast (a, d, g), Savannah (b, e, h) and Sahel (c, f, i) in the study area from 1982 to 2020 for KASS-D (a–c), GPCC (d–f) and CHIRPS (g–i). Broken red and black lines represent the annual long-term mean of the percentage contribution of intense 3- and 5-day wet spells to annual rainfall while the broken blue line depicts the climatological mean of annual rainfall. [Colour figure can be viewed at wileyonlinelibrary.com]

(Figure 13f). Panthou et al. (2014) also reported an increase in the percentage of annual rainfall from extreme events in the central Sahel over different decades but more from daily extremes.

Despite variations in the contribution patterns, datasets generally agree on the trends of intense wet spells during dry and wet periods. In the 1980s, a drought period (Nicholson et al. 2012), the contribution of 3- and 5-day intense wet spells was below the long-term mean, particularly in the Savannah and Sahel. This trend persisted in the Guinea Coast and Savannah into the late 1980s and mid-1990s, respectively, before surpassing the long-term mean. The same pattern occurred during the dry periods of 2000–2005 and 2012–2015, with significant decreases over the Guinea Coast and lesser impacts in the Savannah and Sahel. Notably, from 2006 to 2010, all datasets consistently show an increase in the percentage contribution of intense wet spells above the long-term mean during the wet period when annual rainfall was higher than the long-term mean.

The Mann–Kendall trend analysis (Table S1) reveals a robust and statistically significant increasing contribution of both 3-day and 5-day intense wet spells to annual rainfall across all climatic zones in KASS-D, with the strongest signals observed in the Sahel. While over the Guinea Coast, Kpanou et al. (2020) attributed the observed increase in annual rainfall primarily to a rising frequency of daily extreme events, our analysis shows that the Guinea Coast has experienced the lowest increase in the contribution of 3–5 day intense wet spells to annual rainfall. GPCC similarly shows increasing but weaker trends, particularly in the Guinea Coast and Savannah, though the 5-day spells in the Savannah and Sahel exhibit no significant change. In contrast, CHIRPS demonstrates limited agreement, with mostly non-significant or even decreasing trends, especially over the Savannah. These results further underscore the sensitivity of trend detection in the contribution of intense rainfall events to the choice of rainfall dataset, highlighting KASS-D's stronger capacity to capture long-term intensification of multi-day extreme rainfall events due to higher gauging network density.

5 | Summary and Conclusion

We analysed intense multi-day wet spells in West Africa from 1982 to 2020 using rain gauge and gauge-corrected satellite data. KASS-D data was interpolated from 239 rain gauge stations to a 1° ×1° grid using SPHEREMAP and compared with GPCC, CHIRPS, IMERG and the arithmetic mean of stations within a pixel using Q–Q plots. Wet days were separated from dry days using a 1.0 mm threshold, and 3-day and 5-day events were accumulated with conditions of two and three minimum wet days, respectively, without consecutive dry days. Intense events were defined as those exceeding the 90th percentile of 3-day and 5-day accumulation values at each grid point. Thereafter, we examined the long-term mean spatial distribution, seasonal and inter-annual variability of 3-day and 5-day intense events across the Guinea Coast, Savannah and Sahel. We classified these events into small, mid- and large sizes, assessed their variability, and analysed their contribution to annual rainfall. The key conclusions are as follows:

i. GPCC, compared to KASS-D, shows higher extreme values in upper quantiles, while CHIRPS shows higher

values in lower quantiles. KASS-D interpolated using the SPHEREMAP method almost matches the arithmetic mean of stations when there are 1 to 4 stations per pixel, but its quantile values rise with more than 4 stations.

ii. 3-day and 5-day 90th percentile values and intense wet spells vary latitudinally, peaking over the Guinea Coast and Cameroon highlands and being lowest in the Sahel.

iii. Intense 3-day wet spells tend to be subsets of intense 5-day wet spells, peaking in June and September for Guinea Coast and August for both Savannah and Sahel. Frequency of these wet spells varies across the zones.

iv. From 1982 to 2020, a statistically significant increase has occurred in the annual frequency of intense multi-day wet spells over the study domain and its climatic zones only for KASS-D likely due to its underlying higher number of stations compared to the second station-based product GPCC.

v. Frequency of small-size intense wet spells has decreased, while large-size events have increased. Average size of 3-day and 5-day spells revealed a robust statistically significant increase over time among all the rainfall products. Maximum size of intense 3-day wet spells has also increased significantly.

vi. Over the study period, the percentage contribution of 3-day and 5-day intense events to annual rainfall amounts has increased in all climatic zones, with the highest increase occurring in the Sahel, while the Guinea Coast has the lowest proportion of contribution.

The overestimation of upper quantile values shown by GPCC and lower quantiles by CHIRPS has also been reported by Sanogo et al. (2022) and Gbode et al. (2022). This could be attributed to station density, distance between gauging stations and grid nodes, influence of neighbouring stations with extremely low/high values (Thiemig et al. 2021; Schamm et al. 2014; Becker et al. 2013) in addition to the CHIRPS algorithm. Reduced rain gauge station density increases uncertainty in area mean rainfall, and higher rainfall amounts at individual stations can be smoothed out (Schamm et al. 2014) depending on the number of stations per pixel. GPCC's higher extreme values may be due to fewer stations per pixel compared to KASS-D, which has more stations per pixel on a daily timescale, thus leading to more accurate rainfall representation. Furthermore, the higher station density in KASS-D compared to GPCC has likely unveiled the statistically significant upward trend in the occurrence frequency of multi-day wet spells over the course of the study period, stressing the need to tackle the issue of large-scale data paucity in West Africa.

All rainfall products show meridional variation in the spatial distribution of 90th percentile values and the frequency of 3-day and 5-day intense wet spells, with a higher magnitude along the Guinea Coast extending to the Cameroon highlands. However, zonal variations differ widely and are consistent with findings by Masunaga et al. (2019) and Sun et al. (2018). KASS-D and GPCC exhibit similar spatial distributions due to shared gauge stations and interpolation methods. Becker et al. (2013) and Schamm et al. (2014) claim that GPCC uses a modified SPHEREMAP method that remained valid for dense data regions but relaxed to the SPHEREMAP method in sparse areas like West Africa in practice. CHIRPS and IMERG show smoother 90th percentile distributions compared to gauge-based KASS-D and GPCC, because IMERG uses monthly rainfall values for gauge calibration and the underlying climatology (CHIPclim) in CHIRPS. IMERG's higher rainfall intensity at the southern coast compared to CHIRPS is due to the PMW sensor's tendency to overestimate rainfall in active convective areas and its improved spatial and temporal resolution (Nicholson et al. 2021; Dezfuli et al. 2017).

Seasonal occurrence of 3-day and 5-day intense wet spells follows a monthly variation pattern of rainfall over the three climatic zones of West Africa. The bimodal pattern displayed within the Guinea Coast that peaks in June and August and the unimodal pattern in the Savannah and Sahel, highest in August by all the rainfall products, can be linked to the latitudinal position of the rain-belt within the time of oscillation in each zone (Paeth et al. 2011; Nicholson 2013). As a result of the northward and southward displacement of ITD and its active weather zone to the south, it traverses twice the Guinea Coast and once over other zones, leading to the pattern observed over each zone. Likewise, relatively slow-moving northern (13° N) cyclonic and southern (5° N) anti-cyclonic vortices separated by westerly wind anomaly have been linked to multi-day wet spells (Knippertz et al. 2017; Vondou et al. 2025 (submitted to *Quarterly Journal of the Royal Meteorological Society*, under review)). However, there is limited information on what triggers extreme rainfall beyond the 24-h timescale over West Africa.

Despite the 1980s drought, which saw rainfall drop to about 60% below the long-term mean (Nicholson 2013; L'Hôte et al. 2002) and the ongoing debate over its end (Ali and Lebel 2008), the frequency of intense multi-day wet spells has increased across the study domain. While 3-day and 5-day intense events were generally low during the dry years of the 1980s and early 1990s, they spiked in notably wet years like 1994, 1999 (Nicholson et al. 2012; Panthou et al. 2014) and during wet periods in 2007–2011 in the Guinea Coast and Savannah, and 2003, 2012 and 2020 in the Sahel. Despite debates about the link between rainfall events and inter-annual variability (Nicholson et al. 2012), intense multi-day wet spells remain most frequent during peak rainy seasons, influencing annual rainfall amounts (Lélé and Lamb 2010; Bell and Lamb 2006). Intense 3-day (5-day) wet spells' percentage contribution to annual rainfall has increased by 9% (9%), 16% (14%) and 20% (20%) over the Guinea Coast, Savannah and Sahel, respectively. This suggests that while daily events are crucial, their contribution gradually declines in favour of multi-day wet spells.

While the results of this study highlight a significant increasing trend in the occurrence and size of intense multi-day wet spells shown by KASS-D and were partly captured by other datasets, it further stresses the importance of using multiple sources of quality data in investigating wet spells over data sparse regions like West Africa. However, further work needs to assess how the characteristics of intense multi-day wet spells may change under climate change to inform climate change risk management, adaptation and mitigation strategies.

Author Contributions

Oluwaseun. W. Ilori: conceptualization, methodology, formal analysis, investigation, visualization, writing – review and editing, writing – original draft, validation, data curation. **Marlon Maranan:** conceptualization, supervision, methodology, validation, writing – review and editing. **Andreas H. Fink:** conceptualization, data curation, funding acquisition, supervision, writing – review and editing. **Zachariah D. Adeyewa:** conceptualization, supervision.

Acknowledgements

The first author acknowledges the support of the staff of the Climate Change and West Africa Climate Systems Programme, West African Science Service Centre on Climate Change and Adapted Land Use (WASCAL CC & WACS), Federal University of Technology Akure, Akure, Nigeria. The second and third authors acknowledge funding from the BMBF projects FURIFLOOD (Current and future risks of urban and rural flooding in West Africa—An integrated analysis and eco-system-based solutions; grant no. 01LG2086A) and NetCDA (German Academic Network for Capacity Development in Climate Change Adaptations in Africa; grant no. 01LG2301E). Open Access funding enabled and organized by Projekt DEAL.

Funding

This research is part of a doctoral research project funded by the German Federal Ministry of Education and Research (BMBF) and implemented by the West African Science Service Centre on Climate Change and Adapted Land Use (WASCAL), and Federal University of Technology, Akure (FUTA), Nigeria.

Conflicts of Interest

The authors declare no conflicts of interest.

Data Availability Statement

GPCC, IMERG and CHIRPS datasets used in this study are publicly available from the data creator's repositories. The KASS-D database is operated by the Karlsruhe Institute of Technology.

References

Afiesimama, E. A., J. S. Pal, B. J. Abiodun, W. J. Gutowski, and A. Adedoyin. 2006. "Simulation of West African Monsoon Using the RegCM3. Part I: Model Validation and Interannual Variability." *Theoretical and Applied Climatology* 86, no. 1–4: 23–37. https://doi.org/10.1007/s00704-005-0202-8.

Ageet, S., A. H. Fink, M. Maranan, et al. 2022. "Validation of Satellite Rainfall Estimates Over Equatorial East Africa." *Journal of Hydrometeorology* 23, no. 2: 129–151. https://doi.org/10.1175/jhm-d-21-0145.

Alexander, L. V., H. J. Fowler, M. Bador, et al. 2019. "On the Use of Indices to Study Extreme Precipitation on Sub-Daily and Daily Timescales." *Environmental Research Letters* 14, no. 12: 125008. https://doi.org/10.1088/1748-9326/ab51b6.

Ali, A., and T. Lebel. 2008. "The Sahelian Standardized Rainfall Index Revisited." *International Journal of Climatology* 29, no. 12: 1705–1714 Portico. https://doi.org/10.1002/joc.1832.

Beck, H. E., A. I. J. M. van Dijk, V. Levizzani, et al. 2017. "MSWEP: 3-Hourly 0.25° Global Gridded Precipitation (1979–2015) by Merging Gauge, Satellite, and Reanalysis Data." *Hydrology and Earth System Sciences* 21, no. 1: 589–615. https://doi.org/10.5194/hess-21-589-2017.

Becker, A., P. Finger, A. Meyer-Christoffer, et al. 2013. "A Description of the Global Land-Surface Precipitation Data Products of the Global Precipitation Climatology Centre With Sample Applications Including Centennial (Trend) Analysis From 1901–Present." *Earth System Science Data* 5: 71–99. https://doi.org/10.5194/essd-5-71-2013.

Bell, M. A., and P. J. Lamb. 2006. "Integration of Weather System Variability to Multidecadal Regional Climate Change: The West African Sudan–Sahel Zone, 1951–98." *Journal of Climate* 19, no. 20: 5343–5365. https://doi.org/10.1175/jcli4020.1.

Biasutti, M. 2013. "Forced Sahel Rainfall Trends in the CMIP5 Archive." *Journal of Geophysical Research: Atmospheres* 118, no. 4: 1613–1623 Portico. https://doi.org/10.1002/jgrd.50206.

Casse, C., M. Gosset, C. Peugeot, et al. 2015. "Potential of Satellite Rainfall Products to Predict Niger River Flood Events in Niamey." *Atmospheric Research* 163: 162–176. https://doi.org/10.1016/j.atmosres.2015.01.010.

Chagnaud, G., G. Panthou, T. Vischel, and T. Lebel. 2022. "A Synthetic View of Rainfall Intensification in the West African Sahel." *Environmental Research Letters* 17, no. 4: 044005. https://doi.org/10.1088/1748-9326/ac4a9c.

Crétat, J., E. K. Vizy, and K. H. Cook. 2014. "The Relationship Between African Easterly Waves and Daily Rainfall Over West Africa: Observations and Regional Climate Simulations." *Climate Dynamics* 44, no. 1–2: 385–404. https://doi.org/10.1007/s00382-014-2120-x.

Cullmann, J., M. Dilley, P. Egerton, et al. 2020. 2020 State of Climate Services, Risk Information and Early Warning Systems. In EGU General Assembly Conference Abstracts.

Dezfuli, A. K., C. M. Ichoku, K. I. Mohr, and G. J. Huffman. 2017. "Precipitation Characteristics in West and East Africa From Satellite and in Situ Observations." *Journal of Hydrometeorology* 18: 1799–1805. https://doi.org/10.1175/JHM-D-17-0068.1.

Di Baldassarre, G. D., A. Montanari, H. Lins, D. Koutsoyiannis, L. Brandimarte, and G. Bl¨oschl. 2010. "Flood Fatalities in Africa: From Diagnosis to Mitigation." *Geophysical Research Letters* 37: L22402. https://doi.org/10.1029/2010GL045467.

Diallo, I., F. Giorgi, A. Deme, M. Tall, L. Mariotti, and A. T. Gaye. 2016. "Projected Changes of Summer Monsoon Extremes and Hydroclimatic Regimes Over West Africa for the Twenty-First Century." *Climate Dynamics* 47: 3931–3954.

Dos Santos, S., J.-P. Peumi, and A. Soura. 2019. "Risk Factors of Becoming a Disaster Victim. The Flood of September 1st, 2009, in Ouagadougou (Burkina Faso)." *Habitat International* 86: 81–90. https://doi.org/10.1016/j.habitatint.2019.03.005.

Elagib, N. A., I. Sabry Al Zayed, S. A. Gayoum Saad, M. I. Mahmood, M. Basheer, and A. H. Fink. 2021. "Debilitating Floods in the Sahel Are Becoming Frequent." *Journal of Hydrology* 599: 126362. https://doi.org/10.1016/j.jhydrol.2021.126362.

Fiebrich, C. A., and K. C. Crawford. 2001. "The Impact of Unique Meteorological Phenomena Detected by the Oklahoma Mesonet and ARS Micronet on Automated Quality Control." *Bulletin of the American Meteorological Society* 82, no. 10: 2173–2187. https://doi.org/10.1175/1520-0477(2001)082.

Fink, A. H., and A. Reiner. 2003. "Spatiotemporal Variability of the Relation Between African Easterly Waves and West African Squall Lines in 1998 and 1999." *Journal of Geophysical Research-Atmospheres* 108, no. D11. https://doi.org/10.1029/2002jd002816.

Finney, D. L., J. H. Marsham, D. P. Rowell, et al. 2020. "Effects of Explicit Convection on Future Projections of Mesoscale Circulations, Rainfall, and Rainfall Extremes Over Eastern Africa." *Journal of Climate* 33, no. 7: 2701–2718. https://doi.org/10.1175/jcli-d-19-0328.1.

Froidurot, S., and A. Diedhiou. 2017. "Characteristics of Wet and Dry Spells in the West African Monsoon System." *Atmospheric Science Letters* 18, no. 3: 125–131. https://doi.org/10.1002/asl.734.

Funk, C. 2015. "The Climate Hazards Infrared Precipitation With Stations-A New Environmental Record for Monitoring Extremes." *Scientific Data* 2: 150066. https://doi.org/10.1038/sdata.2015.66.

Gbode, I. E., J. D. Intsiful, A. A. Akinsanola, A. T. Abolude, and K. O. Ogunjobi. 2022. *Uncertainties in Daily Rainfall Over West Africa: Assessment of Gridded Products and Station Gauges*, 65–82. Elsevier. https://doi.org/10.1016/b978-0-323-88456-3.00003-4.

Gosset, M., M. Alcoba, R. Roca, S. Cloché, and G. Urbani. 2018. "Evaluation of TAPEER Daily Estimates and Other GPM-Era Products Against Dense Gauge Networks in West Africa, Analysing Ground Reference Uncertainty." *Quarterly Journal of the Royal Meteorological Society* 144, no. S1: 255–269. Portico. https://doi.org/10.1002/qj.3335.

Han, F., K. H. Cook, and E. K. Vizy. 2019. "Changes in Intense Rainfall Events and Dry Periods Across Africa in the Twenty-First Century." *Climate Dynamics* 53, no. 5–6: 2757–2777. https://doi.org/10.1007/s00382-019-04653-z.

Hastings, D. A., and Coauthors. 1999. "The Global Land One- Kilometer Base Elevation (GLOBE) Digital Elevation Model, Version 1.0." NOAA National Geophysical Data Centre. https://www.ngdc.noaa.gov/mgg/topo/globe.html.

Huffman, D. T., D. Bolvin, D. Bolvin, K. Braithwaite, K. Hsu, and R. Joyce. 2020. "NASA Global Precipitation Measurement (GPM) Integrated Multi-Satellite Retrievals for GPM (IMERG) – Algorithm Theoretical Basis Document (ATBD), Version 6.3." https://gpm.nasa.gov/sites/default/files/2020-05/IMERG_ATBD_V07.pdf.

Jones, P. W. 1999. "First- and Second-Order Conservative Remapping Schemes for Grids in Spherical Coordinates." *Monthly Weather Review* 127, no. 9: 2204–2210. https://doi.org/10.1175/1520-0493(1999)127.

Kendall, M. G. 1975. *Rank Correlation Methods*. E. Arnold.

Kendon, E. J., R. A. Stratton, S. Tucker, et al. 2019. "Enhanced Future Changes in Wet and Dry Extremes Over Africa at Convection-Permitting Scale. Nature." *Communications* 10, no. 1. https://doi.org/10.1038/s41467-019-09776-9.

Kidd, C., and V. Levizzani. 2011. "Status of Satellite Precipitation Retrievals." *Hydrology and Earth System Sciences* 15: 1109–1116. https://doi.org/10.5194/hess-15-1109-2011.

Knippertz, P., A. H. Fink, A. Deroubaix, et al. 2017. "A Meteorological and Chemical Overview of the DACCIWA Field Campaign in West Africa in June–July 2016." *Atmospheric Chemistry and Physics* 17: 10893–10918. https://doi.org/10.5194/acp-17-10893-2017.

Kpanou, M., P. Laux, T. Brou, E. Vissin, P. Camberlin, and P. Roucou. 2020. "Spatial Patterns and Trends of Extreme Rainfall Over the Southern Coastal Belt of West Africa." *Theoretical and Applied Climatology* 143, no. 1–2: 473–487. https://doi.org/10.1007/s00704-020-03441-8.

Lélé, M. I., and P. J. Lamb. 2010. "Variability of the Intertropical Front (ITF) and Rainfall Over the West African Sudan–Sahel Zone." *Journal of Climate* 23, no. 14: 3984–4004. https://doi.org/10.1175/2010jcli3277.1.

L'Hôte, Y., G. Mahé, B. Somé, and J. P. Triboulet. 2002. "Analysis of a Sahelian Annual Rainfall Index From 1896 to 2000; the Drought Continues." *Hydrological Sciences Journal* 47, no. 4: 563–572. https://doi.org/10.1080/02626660209492960.

Maranan, M., A. H. Fink, P. Knippertz, L. K. Amekudzi, W. A. Atiah, and M. Stengel. 2020. "A Process-Based Validation of GPM IMERG and Its Sources Using a Mesoscale Rain Gauge Network in the West African Forest Zone." *Journal of Hydrometeorology* 21, no. 4: 729–749. https://doi.org/10.1175/jhm-d-19-0257.1.

Massazza, G., M. Bacci, L. Descroix, et al. 2021. "Recent Changes in Hydroclimatic Patterns Over Medium Niger River Basins at the Origin of the 2020 Flood in Niamey (Niger)." *Water* 13: 1659. https://doi.org/10.3390/w13121659.

Masunaga, H., M. Schr¨oder, F. A. Furuzawa, C. Kummerow, E. Rustemeier, and U. Schneider. 2019. "Inter-Product Biases in Global Precipitation Extremes." *Environmental Research Letters* 14: 125016. https://doi.org/10.1088/1748-9326/ab5da9.

Monerie, P.-A., C. M. Wainwright, M. Sidibe, and A. A. Akinsanola. 2020. "Model Uncertainties in Climate Change Impacts on Sahel Precipitation in Ensembles of CMIP5 and CMIP6 Simulations." *Climate Dynamics* 55, no. 5–6: 1385–1401. https://doi.org/10.1007/s00382-020-05332-0.

Nguyen-Xuan, T., T. Ngo-Duc, H. Kamimera, et al. 2016. "The Vietnam Gridded Precipitation (VNGP) Dataset: Construction and Validation." *Scientific Online Letters on the Atmosphere* 12: 291–296. https://doi.org/10.2151/sola.2016-057.

Nicholson, S. E. 2011. *Dryland Climatology*. Cambridge University Press.

Nicholson, S. E. 2013. "The West African Sahel: A Review of Recent Studies on the Rainfall Regime and Its Interannual Variability." *ISRN Meteorology* 2013: 1–32. https://doi.org/10.1155/2013/453521.

Nicholson, S. E., A. K. Dezfuli, and D. Klotter. 2012. "A Two-Century Precipitation Data Set for the Continent of Africa." *Bulletin of the American Meteorological Society* 93: 1219–1231.

Nicholson, S. E., A. H. Fink, and C. Funk. 2018. "Assessing Recovery and Regime Change in West African Rainfall From a 161-Year Record." *International Journal of Climatology* 38: 3770–3786. https://doi.org/10.1002/joc.5530.

Nicholson, S. E., D. Klotter, and A. T. Hartman. 2021. "Lake-Effect Rains Over Lake Victoria and Their Association With Mesoscale Convective Systems." *Journal of Hydrometeorology* 22: 1353–1368. https://doi.org/10.1175/JHM-D-20-0244.1.

Omotosho, J. B., and B. J. Abiodun. 2007. "A Numerical Study of Moisture Buildup and Rainfall Over West Africa." *Meteorology and Applied Climatology* 14, no. 3: 209–225. https://doi.org/10.1002/met11.

Onyutha, C. 2020. "Analyses of Rainfall Extremes in East Africa Based on Observations From Rain Gauges and Climate Change Simulations by CORDEX RCMs." *Climate Dynamics* 54, no. 11–12: 4841–4864. https://doi.org/10.1007/s00382-020-05264-9.

Paeth, H., A. H. Fink, S. Pohle, F. Keis, H. Mächel, and C. Samimi. 2011. "Meteorological Characteristics and Potential Causes of the 2007 Flood in Sub-Saharan Africa." *International Journal of Climatology* 31, no. 13: 1908–1926. Portico. https://doi.org/10.1002/joc.2199.

Panthou, G., T. Lebel, T. Vischel, et al. 2018. "Rainfall Intensification in Tropical Semi-Arid Regions: The Sahelian Case." *Environmental Research Letters* 13: 064013. https://doi.org/10.1088/1748-9326/aac334.

Panthou, G., T. Vischel, and T. Lebel. 2014. "Recent Trends in the Regime of Extreme Rainfall in the Central Sahel." *International Journal of Climatology* 34: 3998–4006. https://doi.org/10.1002/joc.3984.

Parmentier, B., B. J. McGill, A. M. Wilson, et al. 2015. "Using Multi-Timescale Methods and Satellite-Derived Land Surface Temperature for the Interpolation of Daily Maximum Air Temperature in Oregon." *International Journal of Climatology* 35, no. 13: 3862–3878. https://doi.org/10.1002/joc.4251.

Ratan, R., and V. Venugopal. 2013. "Wet and Dry Spell Characteristics of Global Tropical Rainfall." *Water Resources Research* 49: 3830–3841.

Roca, R., P. Chambon, I. Jobard, P.-E. Kirstetter, M. Gosset, and J. C. Berg'es. 2010. "Comparing Satellite and Surface Rainfall Products Over West Africa at Meteorologically Relevant Scales During the AMMA Campaign Using Error Estimates." *Journal of Applied Meteorology and Climatology* 49: 715–731. https://doi.org/10.1175/2009JAMC2318.1.

Roehrig, R., D. Bouniol, F. Guichard, F. Hourdin, and J.-L. Redelsperger. 2013. "The Present and Future of the West African Monsoon: A Process-Oriented Assessment of CMIP5 Simulations Along the AMMA

Transect." *Journal of Climate* 26, no. 17: 6471–6505. https://doi.org/10.1175/jcli-d-12-00505.1.

Roxy, M. K., S. Ghosh, A. Pathak, et al. 2017. "A Threefold Rise in Widespread Extreme Rain Events Over Central India." *Nature Communications* 8, no. 1: 708. https://doi.org/10.1038/s41467-017-00744-9.

Sanogo, S., A. H. Fink, J. A. Omotosho, A. Ba, R. Redl, and V. Ermert. 2015. "Spatio-Temporal Characteristics of the Recent Rainfall Recovery in West Africa." *International Journal of Climatology: A Journal of the Royal Meteorological Society* 35: 4589–4605.

Sanogo, S., P. Peyrillé, R. Roehrig, F. Guichard, and O. Ouedraogo. 2022. "Extreme Precipitating Events in Satellite and Rain Gauge Products Over the Sahel." *Journal of Climate* 35, no. 6: 1915–1938. https://doi.org/10.1175/jcli-d-21-0390.1.

Schamm, K., M. Ziese, A. Becker, et al. 2014. "Global Gridded Precipitation Over Land: A Description of the New GPCC First Guess Daily Product." *Earth System Science Data* 6, no. 1: 49–60. https://doi.org/10.5194/essd-6-49-2014.

Schulzweida, U. 2023. "CDO User Guide (2.3.0)." Zenodo. https://doi.org/10.5281/zenodo.10020800.

Shepard, D. 1968. "A Two-Dimensional Interpolation Function for Irregularly Spaced Data." In *Proceedings of the 1968 23rd ACM National Conference*, Brandon/Systems Press, Princeton, NJ, 517–524.

Sultan, B., D. Defrance, and T. Iizumi. 2019. "Evidence of Crop Production Losses in West Africa due to Historical Global Warming in Two Crop Models." *Scientific Reports* 9, no. 1: 12834. https://doi.org/10.1038/s41598-019-49167-0.

Sun, Q., C. Miao, Q. Duan, H. Ashouri, S. Sorooshian, and K.-L. Hsu. 2018. "A Review of Global Precipitation Data Sets: Data Sources, Estimation, and Intercomparisons." *Reviews of Geophysics* 56: 79–107. https://doi.org/10.1002/2017RG000574.

Sylla, M. B., F. Giorgi, E. Coppola, and L. Mariotti. 2013. "Uncertainties in Daily Rainfall Over Africa: Assessment of Gridded Observation Products and Evaluation of a Regional Climate Model Simulation." *International Journal of Climatology* 33: 1805–1817. https://doi.org/10.1002/joc.3551.

Tan, J., G. J. Huffman, D. T. Bolvin, E. Nelkin, and R. Joyce. 2022. "Major Changes to the IMERG Algorithm From V06 to V07."

Thiemig, V., G. N. Gomes, J. O. Skøien, et al. 2021. *EMO-5: A High-Resolution Multi-Variable Gridded Meteorological Data Set for Europe*. https://doi.org/10.5194/essd-2021-339.

Vogel, P., P. Knippertz, A. H. Fink, A. Schlueter, and T. Gneiting. 2018. "Skill of Global Raw and Postprocessed Ensemble Predictions of Rainfall Over Northern Tropical Africa." *Weather and Forecasting* 33: 369–388. https://doi.org/10.1175/WAF-D-17-0127.1.

Vollmert, P., and A. H. Fink. 2003. "Ghana Dry Zone und 'Dahomey Gap': Ursachen für eine Niederschlagsanomalie im tropischen Westafrika." *Die Erde* 134, no. 4: 375–393.

Vondou, D. A., M. Maranan, A. H. Fink, and P. Knippertz. 2025. "Meteorological Conditions Leading to a Catastrophic, Rain-Induced Landslide in Cameroon in October 2019." *Quarterly Journal of the Royal Meteorological Society* Portico. https://doi.org/10.1002/qj.70066.

Willmott, C. J., and S. M. Robeson. 1995. "Climatologically Aided Interpolation (CAI) of Terrestrial Air Temperature." *International Journal of Climatology* 15: 221–229. https://doi.org/10.1002/joc.3370150207.

Willmott, C. J., C. M. Rowe, and W. D. Philpot. 1985. "Small-Scale Climate Maps: A Sensitivity Analysis of Some Common Assumptions Associated With Grid-Point Interpolation and Contouring." *American Cartographer* 12: 5–16.

Yue, S., and C. Wang. 2004. "The Mann-Kendall Test Modified by Effective Sample Size to Detect Trend in Serially Correlated Hydrological Series." *Water Resources Management* 18: 201–218. https://doi.org/10.1023/B:WARM.0000043140.61082.60.

Supporting Information

Additional supporting information can be found online in the Supporting Information section. **Figure S1:** January–December monthly rainfall amount from GPCC provided interpolation test data (ITD) (https://opendata.dwd.de/climate_environment/GPCC/interpolation_test_dataset/) for the year 1988. **Figure S2:** Output of SPHEREMAP configuration used, tested with GPC provided monthly station interpolation test dataset for the year 1988. **Figure S3:** Difference in 90th percentage values between KASS-D and other three rainfall products. **Figure S4:** Pattern correlation of annual frequency of 3-day and 5-day intense wet spells among the three datasets (KASS-D, GPCC and CHIRPS) over the whole domain. This correlation matrix refers to Figure 8. **Figure S5:** Pattern correlation of annual frequency of 3-day (a–c) and 5-day (d–f) intense wet spells amount the three datasets (KASS-D, GPCC and CHIRPS) over Guinea Coast, Savannah and Sahel as indicated on the plot. This correlation matrix refers to Figure 10. **Figure S6:** Linear correlation coefficients between KASS-D (reference) and other rainfall products (GPCC and CHIRPS) for small, mid- and large-sized 3-day (left panels) and 5-day (right panels) intense wet spells. This correlation matrix refers to Figure 11. **Figure S7:** Correlation of average size and maximum size of 3- and 5-day intense events among the three datasets (KASS-D, GPCC and CHIRPS). This correlation matrix refers to Figure 12. **Table S1:** Modified Mann–Kendall trend test result for different sizes of 3-day and 5-day intense multi-day wet spells over the study domain. **Table S2:** Modified Mann–Kendall trend test result for the annual average size of 3-day and 5-day intense multi-day wet spells over the study domain. **Table S3:** Modified Mann–Kendall trend test result for the annual maximum size of 3-day and 5-day intense multi-day wet spells over the study domain. The bold *p*-value indicates a statistically significant trend at a 0.05 significant level. **Table S4:** Mann–Kendall trend test result for the contribution of 3-day and 5-day intense multi-day wet spells to annual rainfall over the three climatic zones in the study domain.